LOGAN RESOURCES LTD.

GRAVITY & INDUCED POLARIZATION SURVEYS AT THE SHELL CREEK PROPERTY, CENTRAL YUKON TERRITORY

Mike Power M.Sc. P. Geoph.

Location: 64° 35' N 140° 25' W
NTS: 116 C 9/10
Mining District: Dawson, YT
Date: November 12, 2005

SUMMARY

Gravity and induced polarization (IP) surveys were conducted at the Shell Creek Property for Logan Resources Ltd. between June 1 and September 12, 2005. The surveys were conducted to investigate gold-copper mineralization on the property.

The gravity survey covered a total of 60 stations, surveyed with helicopter support. Topographic elevations and station locations were surveyed with differential GPS receivers and elevations are considered accurate to ± 50 cm. The data has been corrected for drift, latitude, Free Air, Bouguer Slab, Bullard B and terrain effects. Terrain effects were removed using a digital elevation model to a distance of at least 3 km from any station. Bouguer anomaly measurements are considered accurate to ±200 mGal accounting for all sources of error.

The gravity survey defined a large 3-4 mGal Bouguer high with a 6 km half-width, running NNW-SSE along an axis north of the exposed mineralization on the property. The gravity data was inverted with a three dimensional finite element model incorporating 200 m by 200 m (plan) x 100 m (deep) density cells. Modeling indicates that the source of the large scale gravity anomaly is a deep-seated density source with an apparent density of 2.87 g/cm^2. There are two shallow density highs south of the main density high, one of which lies on the west end of L3200N.

The IP and resistivity surveys covered a total of 19.8 line-km on four lines. The survey was conducted with the expanding pole-dipole array (proximal infinite) measuring 6 separations at a dipole spacing of 50 m (L3200N and L1E) and 100 m (Lines 2900N and L2000N). The IP survey detected low chargeability and high resistivity on all lines except the west end of L2000N where a coincident chargeability high and resistivity low was detected. This target, centred at L200N 10600W, merits additional investigation.

Table of Contents

List of Figures

1.0 INTRODUCTION

Aurora Geosciences Ltd. was retained by Logan Resources Ltd. to conduct a regional scale gravity survey and property scale induced polarization and resistivity (IP) surveys at the Shell Creek Property in the Dawson Mining District, Yukon Territory. The Shell Creek Property contains copper-gold mineralization hosted in a quartzite bed. The purpose of the surveys was to map locate the source of mineralization on the property.

2.0 LOCATION AND ACCESS

The Shell Creek Property is centred at 64° 35' N 140° 25' W on NTS 116 C 9 & 10 in the northern Yukon Territory (Figure 1). The property is 75 km NW of Dawson City. The property is accessible by helicopter with the nearest charter service available in Dawson City. The southern boundary of the property is close to the Yukon River and is accessible by boat or barge.

3.0 MINERAL PROPERTY

The Shell Creek Property consists of the following mineral claims staked under the Yukon Quartz Mining Act in the Dawson Mining District[1]:

Claim Name	Record Number	Expiry date
SIMBA 1-40	YC21149-YC21188	September 15, 2010
SIMBA 41-70	YC21872-YC21901	October 4, 2010
SIMBA 71-214	YC30279-YC30422	October 4, 2010
SIMBA 215-432	YC32891-YC33108	September 11, 2006
SIMBA 433-488	YC35058-YC35113	September 15, 2006
SIMBA 489-578	YC36210-YC36285	August 11, 2006
NSIMBA 1-64	YC35989-YC36052	June 2, 2006

The claims are owned by Logan Resources Ltd. The location of the gravity survey stations and the IP lines relative to the claim boundaries are shown in Figure 2.

4.0 GEOLOGY AND ECONOMIC MINERALIZATION

[1] Claim information from www.yukonminingrecorder.ca on November 8, 2005

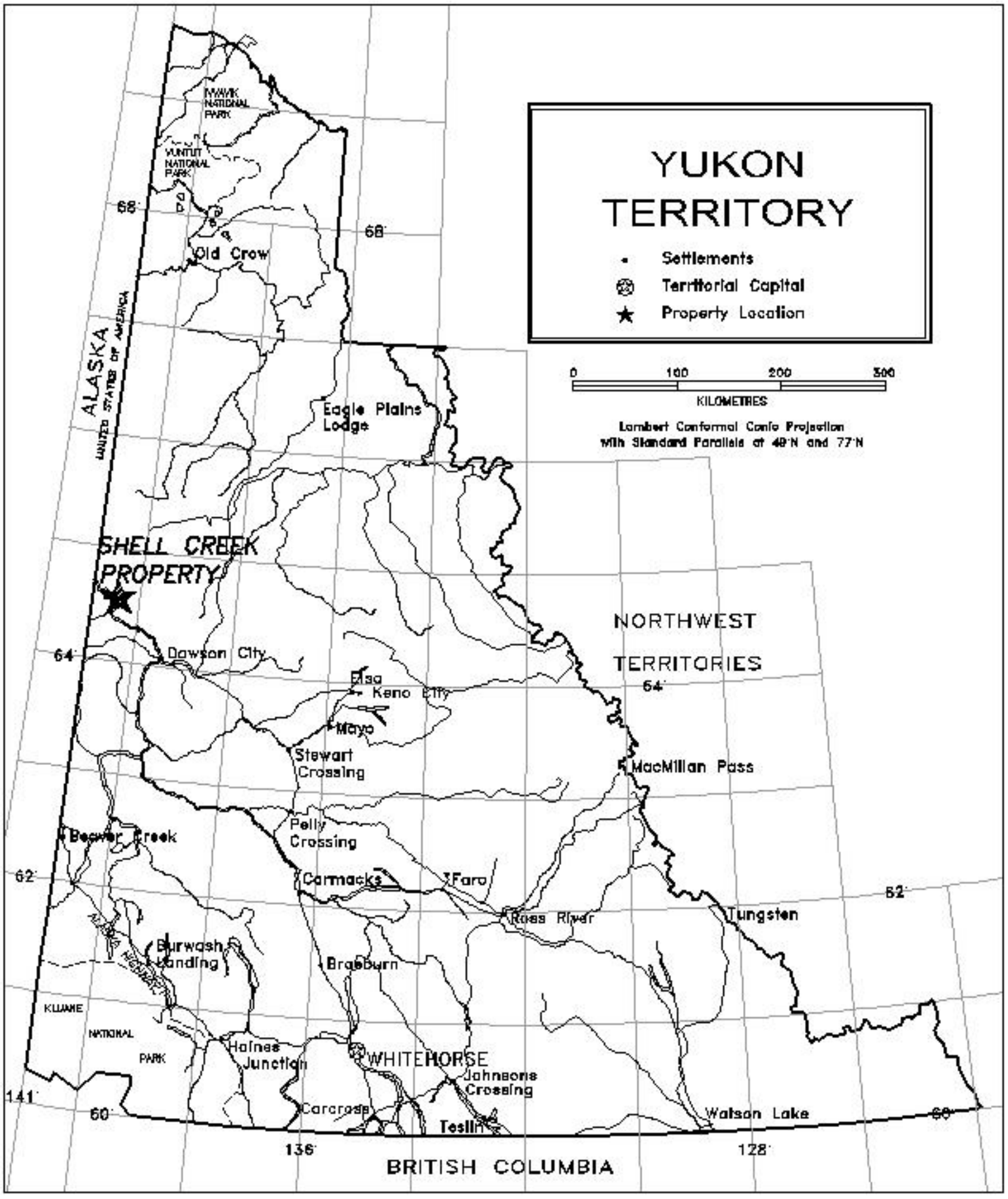

Logan Resources Ltd.	SHELL CREEK PROPERTY	
PROPERTY LOCATION MAP	MINING DISTRICT: DAWSON	
	SCALE 1: 6,000,000	NTS: N/A
	DATUM: N/A	DRAWN BY: DJS
AURORA GEOSCIENCES LTD.	DATE: 10 June 05	FIGURE: 1

The property geology was mapped most recently by Ash (2005) (Figure 3). The property is underlain by Proterozoic Hyland Group rocks and is overlain by unconsolidated Recent sediments in the valley of the Yukon River. From the base to the top of the succession in the property area, the succession consists of limestone (**pCls**), metamorphosed fine grained clastics (**pCs**) and metavolcanic rocks (**pCv**).

Mineralization occurs in banded iron formation within the Hyland Group clastic metasediments and in a series of quartz reefs within the Hyland Group meta volcanics. The quartz reefs are roughly 50 to 75 metres wide, and trend across the region of folded closure. Individual reefs consists of a number of stacked quartz veins that range from less than half a meter, to several meters in thickness separated by intervals of variably chloritized host rock siltstone (Logan Resources, 2005). Visible gold is associated with chalcocite in the quartz reefs.

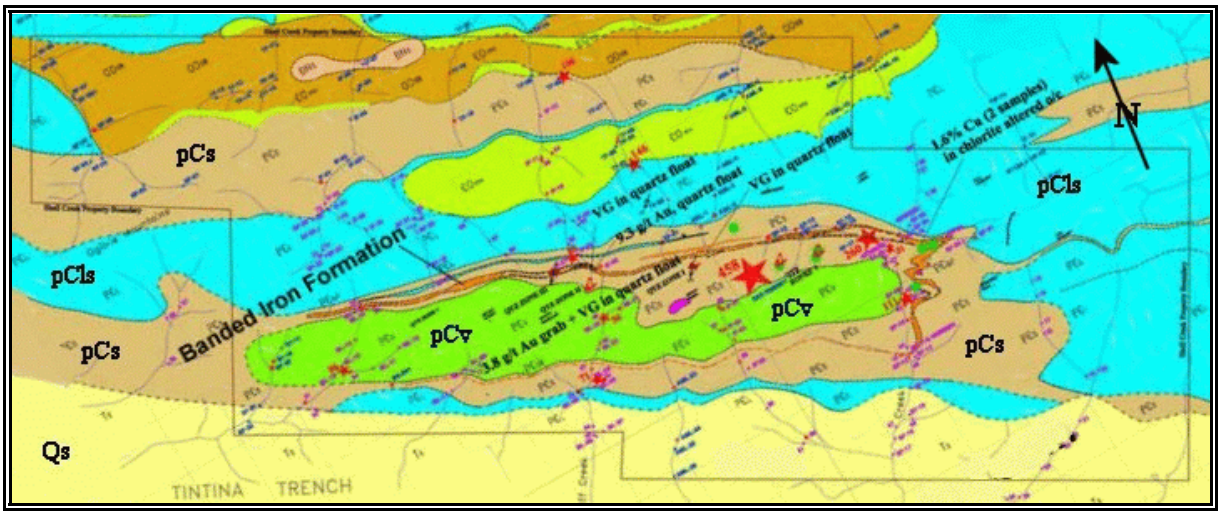

Figure 3. Property geology - Shell Creek Property. (Modified after Ash, 2005).

5.0 GEOPHYSICAL GRID

The gravity survey was conducted in the area shown in Figure 2. A total of 60 stations were surveyed with helicopter support in an area bounded by 515000E 7151000N to 543000E 7176000N (NAD83 / Zone 7N). Stations were sited along traverse lines and in locations with ready helicopter access.

The IP survey was conducted along four lines from 1.4 to 6.3 km long prepared by Logan Resources. Line locations are shown in Figure 4. Mean azimuth (UTM) of the lines surveyed in June was $396^0/116^0$. The lines were being cut at the same time as the IP survey which sometimes adversely affected the IP production. The September IP

line was oriented at 156^0 and covered 1400 m. Total IP production was 19.8 line-km, including re-surveys with different dipole spacings.

6.0 PERSONNEL AND EQUIPMENT

The gravity survey was conducted by the following personnel:

Mike Power, P.Geoph.	Crew chief / geophysicist
Carla Kennedy	Technician

The gravity survey crew was equipped with the following instruments and equipment:

Gravimeter:	Scintrex CG-5 s/n 911009188
GPS base:	Trimble 4000 SSE s/n3535A12121 Antenna 12619 (dual frequency / no ground plane)
GPS rover:	Trimble Pro-XRS s/n 0224005367
Other:	1- Impulse laser range finder (ALG22) 1- P-1.2GHz laptop & colour printer 2 - VHF radios 1 - Jeep SUV

In June, the IP survey was conducted by the following personnel:

Dave Hildes, Ph.D.	Crew chief / geophysicist
Andrea Langerud	Technician
Casey Adshead	Technician
Calvin Delwisch	Helper

In September, the IP survey was conducted by the following personnel:

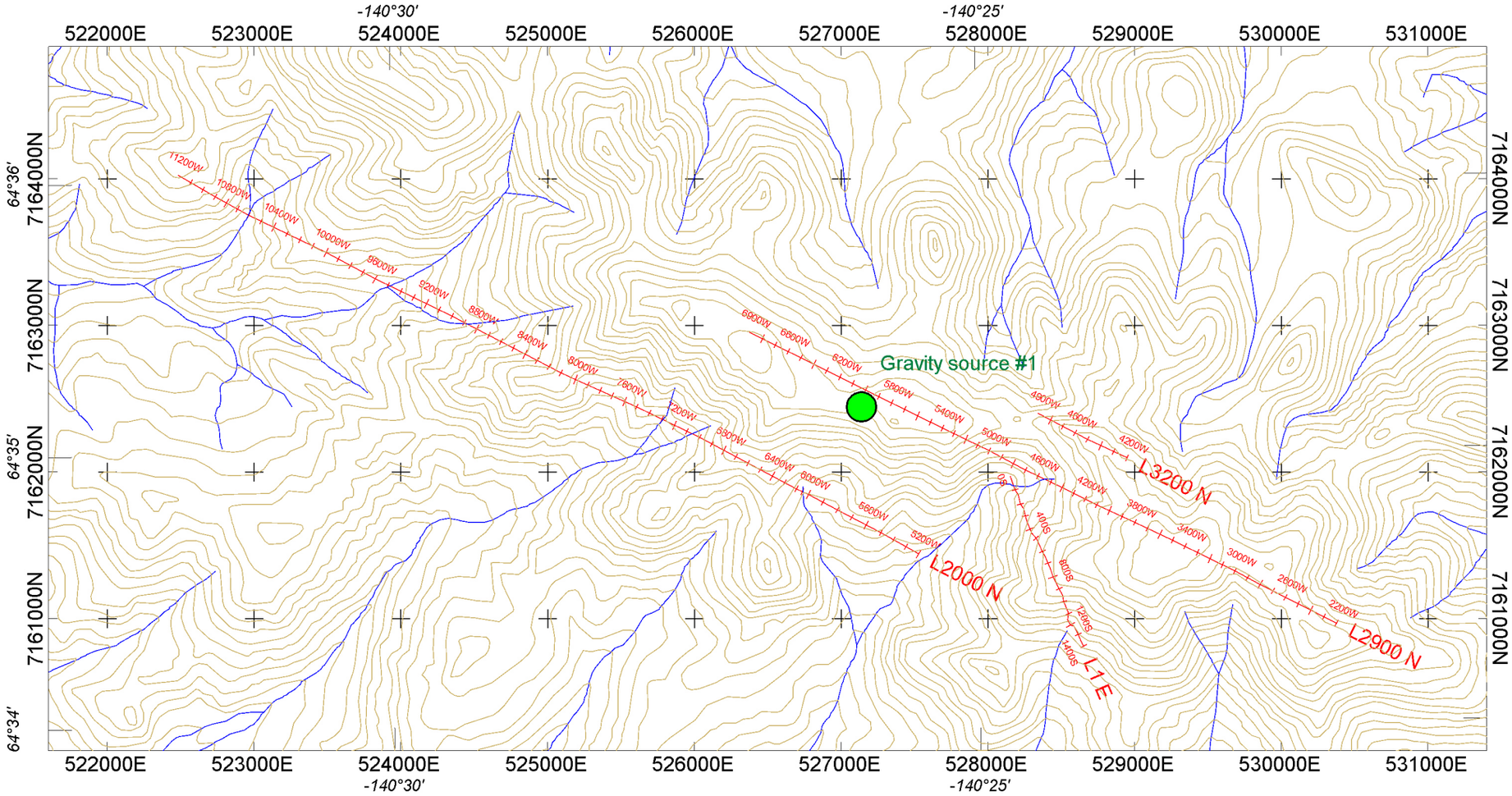

Scale 1:40000

500 0 500 1000 1500 2000

metres

NAD83 / UTM zone 7N

LOGAN RESOURCES LTD.

SHELL CREEK PROJECT
IP SURVEY
Figure 4 - Grid location map

NTS: 116 C 09 & 10
Datum: NAD83 (Canada)
Date: 11 Nov 05

District: Dawson, YT
Projection: UTM Zone 7N
Job: LGR-05-01-YT

AURORA GEOSCIENCES LTD.

Phil Jackson, P. Geoph.	Crew chief / geophysicist
Casey Adshead	Technician
Warren Kapaniuk	Helper
Tobias Schotler	Helper

The IP survey crew was equipped with the following instruments and equipment:

IP Receiver	1 - IRIS Elrec Pro
IP Transmitters	1 - GDD Tx II - 1.4 kW 1 - Honda 5kVA gas generator
Other:	1 - Pentium 4 lap top computer 1 - Ford 1 Ton 1 - Repair tools (electrical / light mechanical) 1 - IP repair tools 1 - Globalstar satellite phone 1 - 4 man summer camp 7 km IP wire, 3 geo-reel winders, 5 geo-reel spools, 2 speedy winders
Software:	Geosoft Oasis 6.0.1 with IP package

The crew was on the property from June 3 to 16, 2005 and from September 11-12, 2005. The survey logs are compiled in Appendix B. Instrument specifications are included in Appendix C.

7.0 GRAVITY SURVEY THEORY

Gravity survey theory is well summarized in Telford *et. al.* (1990). This section describes aspects of gravity survey theory pertinent to the project described in this report.

Gravity surveys measure gravitational acceleration. The force of gravity on between two objects is:

$$F = \frac{GM_1M_2}{r^2}$$

where **F** is the force, G is the universal gravitational constant, M_1 and M_2 are the masses of the two objects and **r** is the distance between them. When the force is normalized against a test mass, the result is the gravitational acceleration (a) due to the second mass:

$$a = \frac{F}{M_1} = \frac{GM_2}{r^2}$$

The acceleration of the test mass is then due to the distribution of the second mass. In the case of a gravity survey, the second mass is the earth and the distribution of mass therein. Explicitly:

$$a = G\int \frac{d \bullet r}{r^3} dv$$

where d is the density, **r** is the radial vector to the mass element and **a** is the acceleration. Gravitational acceleration is measured in Galileos (Gals) where 1 Gal is an acceleration of 1.0 cm/s^2. Average overall gravitational acceleration is 980 Gals and the gravitational acceleration due to targets of interest in the earth's crust are in the order of 10^{-3} (1 milliGal (mGal)) to 10^{-6} (1 microGal (μGal)). Thus a high precision gravity survey measures gravitational acceleration to approximately 1 part in 1 billion.

7.1 Gravity meter function

The Scintrex Autograv gravimeter contains a small test mass suspended by a zero-length fused quartz spring. An electrostatic system is used to maintain the test mass in a constant position where the spring response is linear. Charges are placed on a pair of plates to maintain the test mass in a constant location and the size of this charge (voltage on the plates) will vary with the gravitational force on the test mass. The voltage is converted into a measure of the gravitational acceleration by normalizing the force by the mass of the test mass.

The spring response is a function of force, temperature, air pressure, the inclination of the spring relative to the earth's gravitational field and a slow change in spring constant (instrument drift). Since the force of gravity on the test mass is the quantity to be measured, the remaining influences must be mitigated. The temperature in the spring housing is maintained at a constant value in excess of 45^0 C by a thermostatically controlled heating element. This avoids drift due to changes in temperature. The effect of air pressure is minimal provided the instrument is not operated over a wide range of elevations and changes due to weather are not significant. Instrument inclination may

vary during the course of a measurement because of tripod settling. The Autograv measures the vertical component of the gravity field and as the housing moves off true vertical, the apparent gravity acting on the test mass is reduced. At angles near the vertical, this effect is small and linear, and electronic compensation using a sensitive tilt sensor is used to correct the gravity data for this effect. Instrument drift cannot be totally removed through instrument design but the Autograv eliminates much of the instrument drift by using a correction algorithm. Repeated measurements over a minimum 24 hour period are used to determine an average linear daily drift and this value is extrapolated to determine the drift at any measurement time within 90 days of the last calibration. This drift value may change over time and the remnant instrument drift is removed by a procedure discussed in a following section.

The gravitational acceleration measured by the gravimeter is not a direct measure of true local gravitational acceleration but is relative to an instrument constant and to the range of acceleration in which the measurement was taken. Gravitational acceleration measured by the gravimeter can be leveled to the Geological Survey of Canada gravity control network by the addition or subtraction of an instrument specific constant determined in the field by taking a gravity reading at a GSC control point and computing a static shift.

7.2 Factors affecting gravity readings

The gravitational acceleration at any point is a function of the earth's mass distribution relative to the gravimeter, the distribution of other extraterrestrial masses and the earth's centrifugal force. The sun and moon exert gravitational forces on the earth evident in the tides and the acceleration due to these sources must be removed to yield the gravitational acceleration due to the earth alone. The elevation of the instrument above the ground surface exerts a strong control on the gravitational acceleration. The closer the gravimeter is to masses within the earth, the greater the gravitational acceleration. If mass lies above the gravimeter, however, this will tend to reduce the gravitational acceleration by exerting an upwards force on the test mass. Both effects must be considered. Finally, the centrifugal force of the earth's rotation exerts an upwards force on the test mass in a gravimeter, thereby reducing the earth's gravitational acceleration. This effect varies with latitude and must be removed from gravitational acceleration data. A number of standard corrections are performed to eliminate external sources of acceleration, thereby producing measurements of gravitational acceleration due solely to sources within the earth's crust. The following corrections are commonly applied to the raw gravity data:

1. Drift correction

2. Latitude correction

3. Elevation correction

4. Terrain corrections

These are discussed in turn.

7.3 Drift correction

Repeated gravity readings at a single station show temporal variations caused by solar and lunar gravity (tides), spring hysteresis and atmospheric pressure. Tidal variation is in the order of 30 to 300 μGal per day, instrument drift is in the order of 20 to 200 μGal per day and pressure variations are generally negligible unless there are thunderstorms nearby. In addition to these variations, gravimeters occasionally suffer *tares* or large shifts in base level due to mechanical shock.

To remove the effect of these temporal variations on the final gravity data, the operator establishes one or more gravity base stations and assigns fixed values of the raw gravity to these stations. Prior to, after, and if possible, at several times during each survey day, the operator will reoccupy a gravity base station and take several readings. The difference between the check-in readings and the fixed value (datum) is the instrument drift at the check-in time; this is subtracted from the raw gravity to correct for instrument drift. If tidal corrections are performed with appropriate formulas described below and if there are no tares, the remnant instrument drift is linear and of small amplitude. Consequently, the amount of drift at any station can be calculated by linearly interpolating the drift between bracketing base station measurements using the measurement times of the bracketing base station readings and the measurement time at the field station. A minimum of three base station measurements are required during a long survey day but a gravity base station reading before and after the field readings will suffice on a short day. Large changes in drift indicate that a tares has occurred and the stations between the check-in measurements bracketing the tares must be re-surveyed.

The Autograv calculates tidal drift by applying Longman's (1959) formula taking the gravity station latitude and the reading time as inputs. Because the tidal effects are uniform over large areas at any given time, the Autograv uses a single average latitude value in this calculation. During the same correction, instrument drift is also removed by applying a linear drift correction using constants determined through a cycling experiment described later in this report. Despite this latter correction, there is a small amount of remnant linear instrument drift which must be removed by linear interpolation of drift measured at the gravity base stations during the survey day.

7.4 Latitude correction

Variation in gravitational acceleration due to latitude arises from flattening of the geoid (ie. an increase in distance from the centre of the earth moving towards the equator) and from the effect of centrifugal force when approaching the equator. Both tend to reduce the gravitational acceleration when moving from the poles to the equator. The latitude effect in mGal per km is given by:

$$\Delta G_{Lat} = 0.813 \sin 2\theta - 1.78x10^{-3} \sin 4\theta$$

Latitude effect varies with north-south distance and is greatest at mid-latitudes and least at both the poles and the equator. On small grids, latitude variations are removed by calculating the latitude effect at the centre of the grid and correcting the gravity readings by a variable amount based on their north-south distance from the central station.

7.5 Elevation correction

Three elevation corrections are required. The Free Air effect compensates for the decrease in gravitational attraction resulting from an increase in elevation or, equivalently, an increase in distance from the centre of the earth. Gravity data are normally reduced to an elevation datum below that of the survey. In this case, the Free Air corrected gravity (ΔG_{FA}) is given by:

$$\Delta G_{FA} = 0.3086 * z$$

where z is the elevation of the gravity station above the survey datum. The Bouguer slab correction is next applied to compensate for the upward correction of the material above the gravity survey elevation datum. Were the gravity readings taken on this datum, the material above it would attract the test mass and reduce the measured gravity. The correction is applied by calculating the gravitational effect of an infinite horizontal slab with a thickness equal to the elevation of the gravity station above the datum. Explicitly, this correction (ΔG_B) is:

$$\Delta G_B = -0.0419 \rho z$$

where ρ is the Bouguer density and z is the station elevation. The average crustal density of 2.67 g/cm^3 is normally used in the Bouguer corrected. Finally, an additional correction is necessary to account for the finite nature of the crustal slab used in the Bouguer correction. Obviously a correction based on an infinite horizontal slab is valid only for small elevations above the survey datum and in cases where there is a large variation in topography, the Bouguer correction must itself be corrected for the effect of a finite, curved slab. This correction, the Bullard B correction, is well described by Whitman (1991) and LaFehr(1991b). It is applied to correct the gradient in the Bouguer gravity for the effect of the earth's curvature. The method is applied by using look up tables and applying Bullard-B corrections appropriate to the elevation of the gravity station above mean sea level (LaFehr 1991b). The combined Free Air, Bouguer and Bullard B corrections are combined in a single elevation correction during data

processing. Figure GR-1 illustrates the effect of these corrections.

Some controversy exists concerning the selection of Bouguer density values for the elevation corrections. It has been common practice to adjust the density value away from the average crustal density value in order to minimize effects apparently caused by topography. If an incorrect density were used, the gravity profiles should either follow topography (in the case where the density is too low) or show a negative correlation with topography where the density selected were too high. LaFehr (1991a) recommends the use of the average crustal density (2.67 g/cm^3) in all reductions and the examination of the gravity data to determine the significance of anomalies which are associated with topographic anomalies. This procedure has been followed in performing the elevation corrections described in this report.

7.6 Terrain corrections

Terrain corrections are applied to correct the Bouguer gravity for the upwards gravitational attraction of masses above the station elevation and for the reduction in gravitational acceleration due to an absence of mass in a depression or valley extending below the station elevation. Both of these corrections reduce the elevation corrected gravity. Consequently, terrain corrections are always positive and are added to the gravity data. Terrain corrections are often applied using different algorithms in several zones surrounding the gravity station. The most accurate terrain measurements and algorithms are commonly used for the topography close to the station (near station terrain correction - NSTC) and both the density of data and the accuracy of the approximation algorithms can be decreased at greater distances from the gravity station. Far station terrain corrections are usually applied with digital terrain models (DTMs). A fine DTM and more accurate algorithm is used to calculate terrain effect to within a few kilometres of the gravity station and a coarser DTM and less accurate gravitational approximation algorithm is used at greater distances. LaFehr (1990) recommends terrain corrections be taken to a distance of 160 km surrounding a gravity station and this practice is often used for regional surveys with sparsely spaced stations.

Near station terrain corrections are commonly applied with the sector equation or Kane's Method. This method is based on calculating the gravitational effect of a mass which can be approximated using the equation for the gravitational attraction of a right cylinder. The method is applied using differences in terrain elevation measured in several zones defined by radial distances. Aurora commonly employs standard zones of 2-20 m, 20-50 m and 50-200 m. Each zone is further subdivided into 6 - 60^0 sectors. The gravitational acceleration caused by the excess or deficit mass can be calculated by considering the effect of a pie shaped slice of topography defined by inner and outer radii ($\mathbf{r}_i$ and $\mathbf{r}_o$) and the angle subtended by the slice θ. If ρ is the density, the gravitational effect of that slice $\mathbf{g}_i$ is given by:

$$g_i = \gamma\rho\theta\left\{\left(r_o - r_i\right) + \left(\Delta z^2 + r_i^2\right)^{0.5} - \left(\Delta z^2 + r_o^2\right)^{0.5}\right\}$$

where γ is the universal gravitational constant and $\Delta\mathbf{z}$ is the difference in elevation between that of the sector and that of the station. The terrain effect is the sum of individual terrain corrections in each sector and zone. The NSTC is performed with elevation difference measurements taken by the operator in the field with a clinometer or laser range finder. Visibility limits near station terrain corrections to a distance of about 200 m surrounding the station.

At greater distances, the terrain correction is generally made with DTMs. These consist of an array of nodes to which elevations in metres above mean sea level are assigned. The vast majority of DTM's employ a rectangular distribution of nodes although it is also possible to construct DTM's with triangular node distributions. In general the nodes are uniformly distributed so that each node is square and each node can be considered as an upright prism with a height above mean sea level.

The terrain correction at a gravity station is performed by determining the elevation difference between the top of each node and the gravity station, and then calculating the gravitational effect of the node element. In this calculation, the height of the node element is the difference in elevation between the gravity station and the node top. It is immaterial whether the top of the node is above or below the gravity station as the correction is always positive.

The gravitational effect of the right prism centred at each node can be calculated using a variety of different methods, each of which incorporates some limiting assumptions. The geometry of these methods is sketched in Figure GR-2. Methods commonly applied in order of increasing accuracy include the line mass, Kane's Method, the flat topped right prism approximation (Nagy's Method) and the inclined top right prism method.

At great distances from a station, the dimensions of a node are negligible in comparison to the distance between the node centre and the gravity station. Under these conditions, the gravitational effect of the node-prism can be approximated by a line of mass at a distance r, with cross sectional area s, density ρ and height h as

$$\Delta g = G\rho s\left(\frac{1}{r} - \frac{1}{\sqrt{r^2 + h^2}}\right)$$

A better approximation is to consider each node as a small sector defined by distances to the near and far sides (r_i and r_o), by an elevation difference Δz, and by the angle

which the node subtends at the distance r from the station to the centre of the node (angle θ). With these inputs, the sector equation can be used to calculate the gravitational effect of the node prism (Kane's Method).

A further improvement is to consider the node as a flat-topped rectangular prism at a distance r and at relative coordinates (x,y,z). The coordinates of the prism corner furthest from the gravity station are (x_2, y_2, z_1) and the coordinates of the prism corner nearest the gravity station are (x_1, y_1, z_2). The gravitational attraction of the prism is then:

$$\Delta g = G\rho \left\| x \ln(y+r) + y \ln(x+r) - z \arcsin\left(\frac{z^2 + y^2 + yr)}{(y+r)(y^2+z^2)^{1/2}}\right) \right|_{z_1}^{z_2} \Big|_{y_1}^{y_2} \Big|_{x_1}^{x_2}$$

This relation (Nagy's Method) is used to perform the terrain correction with flat topped prisms. This provides the most accurate, readily calculable approximation to the terrain correction for a topography approximated with a digital terrain model.

One slight approximation remains in the terrain effect calculation. Nagy's Method assumes that the prism has a flat top whereas a more accurate approximation to the true topography would be to construct prisms with inclined tops whose slopes (angle and direction) are determined by the relative elevations of surrounding nodes. This method is numerically challenging and prone to instability; consequently it has not be implemented in the available software.

Upon completion of the terrain corrections, the resulting corrected gravity data is is commonly referred to as the Bouguer Anomaly.

7.7 Bouguer adjustment

The raw gravity readings are made relative to an internal instrument range. The values are correct *relative* to each other across a grid but the absolute values must be levelled to the National Gravity Network. This is performed by re-occupying a government (GSC) gravity station, taking a measurement and then computing a correction factor required to level the survey data to the national network. The field data are then leveled to the national datum by the addition or subtraction of the constant. Care must be taken to apply only those corrections used on the government data to the raw survey data before computing the shift constant. In many cases, GSC data has not been corrected for terrain effect.

7.8 Residual anomaly

The Bouguer anomaly data contains features caused by density variations at various depths. The gravity anomaly caused by a source at an economic depth has a relatively

high spatial frequency anomaly since it arises from a shallow source. The Bouguer anomaly from a larger crustal feature at depth will produce a higher amplitude and lower spatial frequency anomaly. It is common practice to estimate a "regional" Bouguer anomaly due to large scale features not of economic interest and to remove the regional from the Bouguer data, leaving the residual Bouguer anomaly. If properly performed, the residual Bouguer anomaly would be that portion of the gravity field due solely to shallow sources of economic interest.

There are several approaches used in calculating the regional Bouguer anomaly. A simple method is to apply a spatial low-cut filter to the data, removing long wavelength features in the process. In small surveys, regional gradients are sometimes visually estimated and removed from profile data. A third approach is based on the expected signal to noise ratio of the survey. The gravitational effect of the sought-after target can be calculated using modeling software. Given the range of observed drifts, the apparent error in elevations and other sources of error, it is also possible to determine an expected overall accuracy of the gravity survey readings. The gravitational response of the target can then be upward continued until the detectible response falls below the apparent noise level. In other words, the target could not be detected from noise at this height. The gravity data, upward continued to this elevation, can be taken as an estimate of the regional field. The upward continued data is then subtracted from the Bouguer anomaly and the residual data is then largely free from the effect of large, deep sources.

8.0 GPS THEORY

Gravity station elevations must be surveyed in to at least $\pm$ 10 cm in order to produce gravity data accurate to $\pm$ 20 μGal. This can be achieved through spirit level, total station or global position system (GPS) surveys. GPS survey methods were used to determine the elevation of the survey stations in the survey described in this report and this section summarizes the measurement method.

The Navstar Global Positioning System consists of 26 low altitude satellites, a master controlling station in Colorado Springs, CO and three uplink stations in Hawaii, Ascension Island, Diego Garcia and Kwajalein in the western Pacific Ocean. The satellites circle the earth at an altitude of 20,200 km with 4 satellites (space vehicles of Svs) in each of 6 planes inclined at 55^{o} to the equator. Two SV's are spares. Each SV contains an atomic clock and transceiver.

The GPS signal quite complicated and occupies a wide bandwidth in order to nullify jamming. The system fundamental frequency (f_o)is 10.23 MHz. Satellites transmit messages on two carrier frequencies:

L1 carrier - 1575.42 MHz (154 f_o) with a wavelength of 19 cm
L2 carrier - 1227.60 MHz (120 f_o) with a wavelength of 24 cm

Several signals are impressed on the carrier frequencies by amplitude modulation:

Name	Carrier (freq)	Description
Navigation message	L1 & L2 (1500 Hz)	Satellite status, ephemeris and clock corrections
P-Code	L1 (10.23 MHz)	Precision Code: Encrypted pseudorandom noise signal containing clock time signal (time of transmission). The encryption is unclassified and available for civilian use. Pseudorange accuracies with this code are in the order of 30 m.
Y-Code	L1 (10.23 MHz)	Encrypted P or Anti-spoofing (AS) Code: Encrypted pseudorandom noise signal containing clock time signal (time of transmission). The encryption is classified and this signal is for military use. Accuracy of the GPS system with this code is degraded to 100 m but military users can achieve psuedorange accuracies of better than 30 m by removing the encryption.
C/A-code	L1 and L2 (1.023 MHz)	Clear acquisition code: Non-encrypted clock time signal with pseudoranges accurate to $\pm$100 m.

8.1 Positioning

GPS receivers contain an internal clock (oscillator) which is synchronized to GPS time. GPS time is the absolute time standard used for the entire GPS system and is expressed in coordinated universal time (UTC). Each SV has a clock synchronized to GPS time and transmitted clock errors are contained in the navigation message. The C/A and P or Y code transmissions contain the time of transmission from the satellite. Once the GPS receiver has 4 satellites in view, it can come up with a unique solution for the four variables in the position equation: x,y,z and t (time). The receiver generates a best-fit solution to GPS time and synchronizes the receiver clock to GPS time. The phase shift in time between the code signal picked up by the receiver and the internal receiver clock yields the transit time (time of receipt less time of transmission). This time, together with the known propagation velocity of the radio wave yields a pseudorange. The satellite navigation message transmits the satellite ephemeris - a

precise description of the satellite's orbit and thus, its position. Using the ephemerides and pseudoranges, the location of the receiver can be calculated to an accuracy limited by the psuedorange accuracy and the relative geometry of the satellites. GPS positions are accurate to ± 30 m with P-Code and to ± 100 m with C/A Code.

8.2 Differential corrections

The accuracy of GPS positions can be improved by differential processing. A base station GPS is placed on a point whose geographic coordinates are accurately known. The base receiver then tracks the same satellites that are used by a nearby receiver (rover) which is being used to determine an unknown position. The base receiver computes the error in pseudoranges by comparing the apparent pseudorange from the SV's P or C/A code with the known pseudorange computed from the satellite ephemerides and the known base station position. The errors in satellite pseudoranges are then used in either real-time (via radio link) or post-acquisition processing of the rover's position. Differential correction can yield positions accurate to 0.50 m in x, y and z provided the PDOP is acceptable.

8.3 Dilution of precision

The accuracy of a GPS position depends upon both the accuracy of the pseudoranges and the distribution of the satellites relative to the receiver. If the SV's are clustered in one location in the sky, small changes in the pseudoranges will translate into large variations in the station coordinates. In particular, if the SV's are clustered overhead, the error in elevation will be increased. The effect of the SV distribution on the quality of the position measurement is quantified as the "dilution of precision" or DOP. DOP is further subdivided into horizontal (HDOP) and vertical (VDOP). A quantity which describes the overall accuracy of the position measurement considers the length of the error ellipse axes, the largest of which is quantified as the point dilution of precision (PDOP). In general, a PDOP less than 6.0 is considered desirable to achieve accuracies of ± 50 cm in a differential correction.

8.4 Carrier phase processing

GPS positions can be refined further by employing the short wavelength carrier phase to refine the position accuracy. In simplified terms, the method is as follows: A base receiver is set up at a known point and a rover is set up at the point whose position is to be determined. The two receivers then record data from at least 5 SV's in common view for periods of time which depend upon the method being used. Three techniques are in common use:

Static survey	Receivers record each base line for at least 45 minutes. Post processing uses the C/A code and the carrier phase shift to calculate base lines.
Fast static survey	Receivers record each base line for at least 5 minutes and use the P-Code and carrier phase shift to calculate base lines.
Kinematic survey	Both the base station and the rover are set up over a known point and, after a short initialization period, the rover is moved from point to point and base lines are measured for period of 30 to 60 seconds. Both receivers must maintain a lock on the same receivers.

Static surveys can achieve accuracies of 5 mm $\pm$ 5 ppm while Fast Static and kinematic surveys can achieve accuracies of 5 mm $\pm$ 10 ppm. Carrier phase processing requires that the receiver be capable of recording at least 1 carrier phase (single frequency receiver) but better results under a wider variety of operating conditions are possible using receivers capable of receiving both L1 and L2 carriers (dual frequency receivers).

Carrier phase processing uses several techniques to measure base lines. Differentially corrected GPS positions are used to narrow down a range within which possible solutions to the base line equation may be found. Under optimum conditions this would involve a preliminary determination of distance to within 1 to 2 m. To further improve accuracy, the carrier phase difference (phase shift) between the two receivers is considered. The fraction of a wavelength phase difference between the two receivers can be determined very rapidly but the integer number of full wavelengths phase difference between the receivers cannot be readily determined with a single phase difference. This is referred to as the integer ambiguity. In addition, the method has to be able to correct itself if one of the receivers loses contact with one of the satellites and "loses its place" in the signal (cycle-slip). Finally, the processing must account for propagation error caused by unknown velocity variations within the ionosphere. Several methods are used together to remove external sources of error, resolve the integer ambiguity and correct for cycle-slip:

Single difference	Difference in phase between 2 receivers measuring the same satellite over the same interval (epoch). This removes the effect of satellite clock, orbital and atmospheric delays.

Double difference	Difference between 2 single differences. This removes the effect of receiver and satellite clock drift.
Triple difference	Difference over time between 2 double differences. This removes integer ambiguity and resolves cycle-slips.

Combinations of the differences for a large number of readings are solved for a best-fit solution using least-squares methods. Carrier phase processing generates one of several possible types of solutions depending upon the data available:

Float solution	Poor solution as the processor is unable to resolve the integer ambiguity. Errors in the order of 1 wavelength (19 to 24 cm) are possible.
Fixed solution	Good solution; one solution yields integer values significantly better than others. Errors less than 1 wavelength are possible.

Fixed solutions for dual frequency receivers fall into one of three types:

Wide Lane Fixed	Uses L1 and L2 differences, generating a base line solution using a wavelength of 86.2 cm. This is used in long base line surveys.
Narrow Lane Fixed	Uses combinations of L1 and L2 solutions generating a base line solution using a wavelength of 10.2 cm. This solution effectively removes ionospheric effects.
Ionospheric free solution	Best possible solution generated using L1 and L2 to achieve maximum possible accuracy.

8.5 Factors affecting GPS survey accuracy

The relative satellite geometry, signal status and elevation of the satellites above the horizon control the accuracy of a base line determination or of a position fix. Selective Availability (SA) is the military term for the deliberate dithering of the clock signals from the GPS satellites to degrade positional accuracy. A slow variation in position is caused by the introduction of error into the satellite ephemeris in the navigation message and a smaller and much more rapid position error is introduced into the code transmission. This latter effect causes significant errors in velocity determinations. The encryption of P-Code to Y-Code can affect Fast Static surveys since these use the P-Code to

determine the starting position for a base line solution. The user range accuracy (URA) is a measure of the accuracy of a pseudorange. If this number is greater than 30 m, selective availability is probably in effect.

The signal to noise ratio (SNR) is a measure of the strength of the signal relative to background noise. An SNR of at least 6 is required for a decent positional fix or base line solution, common ranges are from 12 to 20.

A minimum of 5 visible (ie. detectable) satellites are required for carrier phase processing and for an accurate differential GPS position. A minimum of 4 SV's is required for routine positioning. A solution with more than 4 satellites is referred to as an over-determined 3D (OD3D) solution.

The relative geometry of the satellites exerts a strong influence on the accuracy of a solution. If all SV's are directly overhead, the generated position solution is relatively insensitive to horizontal error whereas a much tighter solution is possible if the satellites are spread across the sky. The point dilution of precision (PDOP) is a measure of the error in location caused by geometry. Values of 4 or less are good, 5 to 7 are acceptable and greater than 7 is considered very poor.

Multi-path errors are caused by SV signals reflecting off surfaces near the receiving antenna. Multipath errors are a major concern in both differential and carrier phase surveys where reflections near a base station receiver can significantly degrade the quality of the positions and base line solutions. Fortunately they are largely avoidable through care and attention in the field.

9.0 GRAVITY SURVEY SPECIFICATIONS AND FIELD PROCEDURE

The gravity survey was conducted according the following specifications with exceptions as noted:

Instrument preparation: The gravimeter was levelled on a concrete slab and warmed up for a period of 48 hours to stabilize. Thereafter, the instrument was cycled for approximately 12 hours, taking readings for 120 seconds every 10 minutes. Following this, the instrument drift constant was reset using the internal instrument algorithm. As a final check, the instrument was then cycled for 24 hours at the same sampling interval and the drift curve examined to ensure that the instrument was stable. Following calibration, the instrument remained under power at all times.

Horizontal survey datum: NAD 1983 (Canada Mean) with all data projected in UTM Zone 7N coordinates.

Vertical survey datum: EGM96 (Global) (Geoid elevations)

Station marking: Stations were marked with flagged nails.

GPS base station: 526415.666E 7162784.957N (Geoid elevation 1378.9 m ASL). Station location determined by survey from Geodetic Survey of Canada monument #65A44 using prescribed coordinates for this point.

Gravity base station: Two gravity base stations were read each day. The first was located at the Trans North Helicopter hangar. The grid gravity base station was located at the GPS base station and is coincident with the GPS base station hub. The nominal grid gravity base station datum used for all drift corrections was 5079.570 mGal.

Gravity readings: Readings were stacked for 60 s. One reading was taken at each station if the standard deviation was less than 50 μGal. If the gravity readings exceeded this threshold, at least three repeat measurements were collected.

Drift corrections: On the property, drift check-in readings were conducted at the survey gravity base station prior to, during, and following each day's survey at a minimum. In addition, a gravity station was read at the Trans North hangar to serve as an emergency backup in the event that the crew could not check in at the end of the day. Readings at the hangar station are denoted in the dump files as Line 98 / Station 98. Readings at the grid base station are denoted as Line 99 / Station 99.

Base GPS: The base station GPS receiver was cycled using a 10 s epoch (reading interval) as an optimum compromise between memory requirements and rover acquisition time. Base station PDOP masks were set to <25.0, elevation mask to > 2^0 and signal to noise (SNR) ratio mask was set to >2.0. All elevation readings were corrected for antenna height. The base antenna was securely mounted on a fixed tripod throughout the survey.

Rover GPS: Antenna was placed on the gravity survey station hub and elevations were corrected for rover antenna height. A minimum of 30 position measurements were taken per station survey and these were averaged to determine the final station location. Rover elevation, PDOP and SNR masks were set higher than corresponding base station masks to ensure that all rover measurements had matching base station satellite records.

Near station terrain corrections: All stations sites were flat for at least 2 metres. No local terrain measurements were taken and all terrain effect was removed with using the digital terrain model (DTM).

Levelling: The survey was levelled to the GSC gravity network using two GSC gravity locations which are located at station 41 and 51 on the grid. This survey was levelled to the GSC datum by subtracting 5397.000 mGal from the final Bouguer anomaly. The attached spreadsheet (GSC gravity levelling.xls) summarizes the calculations made to determine this value.

10.0 GRAVITY DATA PROCESSING AND REDUCTIONS

Gravity data processing included the following steps and procedures:

1. *GPS processing.* The GPS data was processed with Trimble Pathfinder Office (5.01) using carrier phase and code processing. The nominal GPS base station location cited above was used as the reference position for all station measurements and the antenna heights of the rover and base were checked daily and used in the corrections. The data was exported in UTM NAD 83 (Zone 7N) coordinates with elevations in metres above the ellipsoid height (EGM96 (Global) / NAD83 Geiod).

2. *Position merge.* The gravity data was merged with the GPS data based on common line / station coordinates of readings in each data set.

3. *Drift corrections.* Daily drift files were created from the check-in measurements. The nominal gravity base station reference reading was used in all corrections; the data is corrected to a common datum regardless of the survey day. Drift corrections were applied by linear interpolation between the nearest-in-

time check-in measurements prior to and after the field reading.

4. *Latitude correction.* The latitude correction was applied by calculating the linear gradient in the latitude effect at the centre of the survey area and removing the latitude effect calculated relative to this point. The central point used in the latitude calculation was 528000E 7162000N at a latitude of 64.582^0 N. The effect of the declination between UTM Grid North and True North was removed by adjusting the distance north of the central point using the measured declination of 0.62^0 E.

5. *Elevation corrections.* Free Air, Bouguer Slab and Bullard-B corrections were applied using mean sea level (z=0 m) and a density of 2.67 g/cm^3.

6. *Near station terrain corrections.* No measurements of near station topography were made and no near station terrain corrections were made using local topographic measurements. All terrain corrections were made with a digital elevation model as described below.

7. *Far station terrain corrections.* A digital terrain model was created from the Geodetic Survey of Canada NTS topographic sheet 116C9/10 by extracting the coordinates of contour line segment end points and gridding this data using a 25 m cell size. The DTM extends from 515000E 7151000N to 543000E 7176000N and encompasses an area at least 5 km from any station in the survey area. The far station terrain corrections were applied with an exclusion distance of 25 m. The far station terrain correction algorithm calculates the gravity effect of a flat-topped prism with dimensions equal to the node spacing.

8. Plotting. Maps of the Bouguer Anomaly with terrain and without are included with this report. Digital copies of these plots are included in the digital archive on CD-ROM.

11.0 GRAVITY MEASUREMENT ERROR

This section describes the sources of error present in the data and estimates the overall error in the Bouguer Anomaly after the application of all standard reductions.

11.1 Measurement error

Each gravity reading was stacked 60 times and, if the reading standard deviation exceeded 50 μGal, the reading was repeated three times and averaged. The discrepancies between repeat readings at noisy stations rarely exceeded 20 μGal and this value is taken as a measure of raw measurement error.

11.2 Instrument drift

Gravimeter drift during the course of the survey is shown in the plot below. Average daily drift was in the order of 50 μGal. Error due to incorrectly estimated drift is estimated at no more than 10 μGal.

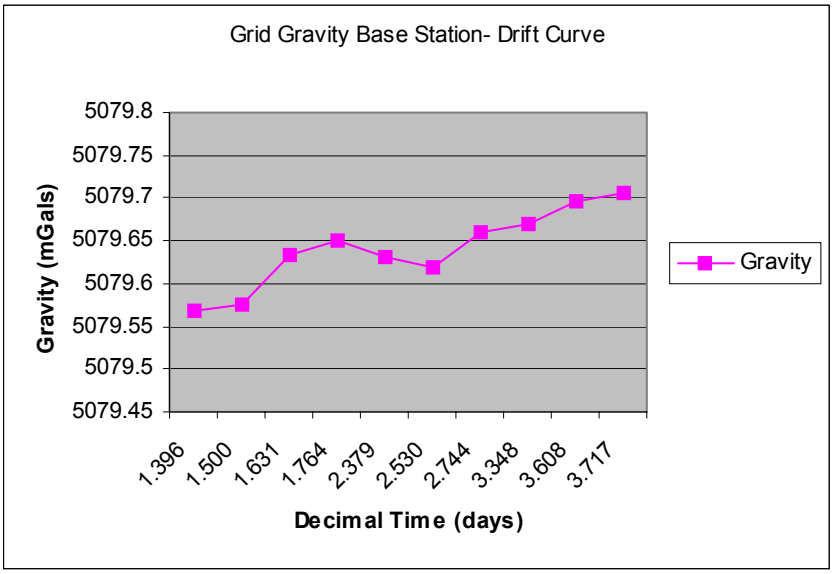

11.3 Elevation error

The crew chief failed to take repeat GPS measurements during the course of the survey. Station 3 however was inadvertently repeated (on June 9 and June 11). The data is summarized below:

Point	UTME	UTMN	Elevation
Point 3 - 09 June 05	528703.986	7162198.554	1372.008
Point 3 - 11 June 05	528704.261	7162197.716	1371.901

This resurvey suggests that the GPS was working satisfactorily. In addition, the GPS indicated elevations of the gravity stations were checked against the indicated elevations of these points on the digital elevation model. It should be noted that the DTM with which these points were compared did not incorporate the GPS elevations themselves but relied upon contour map elevations. Maximum discrepancies in the

order of ± 5 m were noted between the GPS indicated stations elevations and the interpolated elevations of the gravity stations derived from the digital topographic maps. This too suggests that the GPS-derived gravity station elevations are correct. Error in elevation is estimated at no more than ± 50 cm (0.100 mGal).

11.4 Latitude correction error

The latitude correction error is assumed to be negligible given the assumed horizontal accuracy of the station locations (± 50 cm).

11.5 Terrain correction

Errors in far station terrain corrections are due to three sources. These include the effect of the simplified geometry of each DTM node (flat topped prism) and the node size (20 m); errors in the topographic maps from which the DTM was constructed; and round-off error. Errors introduced by the first source are likely minimal given the great distance between the sources (nodes) and the gravity stations. Errors in the topographic maps would likely create small local anomalies - largely single station anomalies in this case. Round-off error is likely not significant as the processing is performed with double precision float variable and rounding errors should in general cancel as there is as much chance of rounding up as rounding down in any calculation. As an approximation, far station terrain corrections errors are assumed to be no more than 5% of the applied far station terrain correction, averaging 57 μGal.

11.6 Global error estimate

The error in the Bouguer Anomaly from all sources is the sum of the errors in each correction and is estimated to be about 200 μGal.

12.0 GRAVITY INVERSION

The gravity data was modelled using the University of British Columbia Geophysical Inversion Facility Grav3D software package. This section describes the inversion methodology and the parameters used to invert and interpret the gravity data.

Starting with a model of the earth consisting of rectangular prism elements (a finite element mesh) with varying dimensions and initial densities, Grav3D iteratively adjusts the densities of each element until the forward modelled response matches the observed gravity within the bounds of measurement error. The program uses a forward modelling subprogram to model the gravity response for a given model, computes the differences between the forward modelled data and the observed data, and adjusts the density of each node using a sensitivity matrix which encapsulates the contribution of

each node to the observed gravity at a given station. At a given station for a given difference between observed and modelled gravity, the adjustment is calculated by adjusting the density of each node by an amount scaled from the sensitivity matrix.

12.1 Forward modelling

For a series of observations **d** = $(d_1, d_2, d_3, \ldots d_i)^T$, and a model with M cells each with a density $\boldsymbol{\rho} = (\rho_1, \rho_2, \rho_3, \ldots \rho_\iota)^T$, the value of the gravity at a given station can be written as the sum of the contributions from the various elements:

$$d_i = \sum_{j=1}^{M} \rho_j G_{ij}$$

where G_{ij} describes the gravitational effect of a prismatic element j to the observation at point i. The gravitational effect of a rectangular prism element is calculated using Nagy's (1966) method. Consider a flat-topped rectangular prism at a distance r and at relative coordinates (x,y,z). The coordinates of the prism corner furthest from the gravity station are (x_2, y_2, z_1) and the coordinates of the prism corner nearest the gravity station are (x_1, y_1, z_2). The gravitational attraction of the prism is then:

$$\Delta g = G\rho \left\| x \ln(y+r) + y \ln(x+r) - z \arcsin\left(\frac{z^2 + y^2 + yr)}{(y+r)(y^2+z^2)^{1/2}}\right) \right|_{z_1}^{z_2} \Big|_{y_1}^{y_2} \Big|_{x_1}^{x_2}$$

The matrix **G** is the sensitivity matrix describing the geometric portion of the gravity contribution of each mesh cell to each of the observation points. In vector notation, a set of observations (d) can be forward modeled by the following relation:

$$d = \mathbf{G}\rho$$

The Grav3D subprogram GZFOR3D generates the sensitivity matrix which in turn can be used to rapidly forward model the gravitational response for a given density model defined by the vector ρ.

12.2 Inversion methodology

The inversion problem can be framed as follows: For a given set of observations, find a model which:

1. Replicates the observed data within the bounds of measurement error.

2. Differs as little as possible from a reference model incorporating whatever is known about the local geology and.

3. Is smooth in three dimensions.

To achieve this end, a model objective function is defined which incorporates these conditions. Grav3D incorporates an objective function defined as follows:

$$\phi_{\mathrm{m}} = \alpha_{\mathrm{s}} \int_V w_s w^2(z)(\rho - \rho_o) dv + \alpha_{\mathrm{x}} \int_V w_x \left(\frac{\partial w(z)(\rho - \rho_o)}{\partial x} \right)^2 dv +$$

$$\alpha_{\mathrm{y}} \int_V w_y \left(\frac{\partial w(z)(\rho - \rho_o)}{\partial y} \right)^2 dv + \alpha_{\mathrm{z}} \int_V w_z \left(\frac{\partial w(z)(\rho - \rho_o)}{\partial z} \right)^2 dv$$

where w_x, w_y, w_s, and w_z are spatially dependent weighting functions and α_x, α_y, α_z, and α_s are coefficients affecting the relative importance of the three different components fo the objective function. The reference model is ρ_0 and the closeness of the reference model to the final model is controlled by w_s. The weighting functions w_x, w_y, and w_z can be used to constrain the final solution to one which is more intense or attenuated in one or another dimension. Finally, w(z) is a depth weighing function which is used to counteract the natural insensitivity of the kernel function **G** with depth. Unchecked, any solution would show most of its variability near surface regardless of the other weighting functions. To overcome this, w(z) is defined in the form:

$$w(z) = (z + z_0)^{-\frac{\beta}{2}}$$

where β and z_0 are defined to ensure that the model generates features at depth. The model objective function in an optimum solution will stabilize around some constant value, indicating convergence. This value will not (and should not) be close to zero unless by coincidence the modeller were to specify a reference model which is almost an exact fit to the data.

Having defined a measure of model acceptability, it is necessary to define a measure of misfit which naturally must be minimized in an acceptable solution. The model norm is calculated as follows:

$$\phi_d = \left\| W_d (d - d^{obs}) \right\|^2$$

where d is the value at a station predicted by the model, and W_d is a diagonal matrix whose elements are the inverse of the standard deviation in the given reading d^{obs}. The

inverse problems can then be restated as follows:

1. Minimize ϕ_m and

2. Minimize ϕ_d to a level determined by the error in the data.

The threshold for ϕ_d in perfectly weighted data would be the number of readings in the data set (N). Since this value may be too tight for noisy data, a chi-factor is defined which is normally 1.0 but can be increased to set the threshold high enough to allow convergence to a minimum value of ϕ_d.

12.3 Depth weighting

Because there is no unique solution to a gravity problem and because the gravitational effect of mass at depth falls off with the square of the distance, inversion models in an unconstrained algorithm consist of small and flat source masses near the surface. It has been found through experimentation that the decay of the gravitational contribution of elements at depth follows a function in the form $(z+z_0)^2$. To remove the effect of depth weighting, we define the w(z) as shown in the previous section. Since w(z) is squared in each term for ϕ_m, it can be expected that for β=2, the effect of depth decay would be compensated completely. In practice however, the inversion produces reasonable models for $\beta \leq 2.0$ and at $\beta \geq 2.0$ the algorithm has been noted to deteriorate in some examples. As a result, the default value of β=1.9 is used in most inversions. The value of z_0 can be determined by matching the function with the field produced by a column of cells directly beneath the observation point. This is the procedure followed automatically in Grav3D.

12.4 Effect of the regional anomaly

Bouguer Anomaly data can be both positive and negative, depending upon the datum selected. It is important to remove the regional field before beginning the inversion in order to isolate the response due solely to the anomalous mass. A data set which exclusively portrays the response of local anomalous masses will invert to yield a model which is most sensitive to the geometry and density of the local anomalous masses. In particular, the sign of the data can matter. Best results with Grav3D generally occur when the polarity of the density is constrained to either entirely negative or positive density values. In order to due this, care must be taken when defining and removing the regional field to ensure that this datum shift does not unintentionally bias the data. Two general procedures are employed. First, the long wavelength regional field should be remove through prediction and subtraction, low cut spatial filtering or upward continuation and subtraction. Secondly, it is worthwhile to boost all anomalous observed gravity values above zero for a positive gravity anomaly and to depress them below zero for a negative gravity anomaly before inverting the data. This will generate a

minimum of large scale deep features created to replicate a residual regional field. For a positive gravity anomaly, positivity may be invoked, restricting the modelling to generating only densities above zero. Similarly, negativity may be invoked in the case of inverting negative gravity anomalies.

13.0 IP SURVEY SPECIFICATIONS

The IP survey was conducted according to the following specifications:

Station locations:	Station spacing was 50 m. Line ends and stations every 500 m were surveyed with non- differential GPS.
IP Array:	Modified pole-dipole array.
Dipole spacing:	25 and 50 m on L3200N 100 m on L2900N 100 m on L2000N
Separations:	Six dipoles were read from n=1,6.
Tx:	Time domain with a 50% duty cycle, reversing polarity, 0.125 Hz.
Parameters read:	M - total chargeability Mi - 20 semi-logarithmically spaced time slice channels V_p - primary voltage Sp - self-potential voltage I - current Rs - electrode resistance Err - standard deviation of stacked readings
Stacks, repeats:	At least 16 stacks were taken at each station. Stations that were noisy (error > 5 mV/V) had extra readings taken to ensure repeatability.

14.0 IP / RESISTIVITY DATA PROCESSING

The following procedures were used to prepare and invert the induced polarization and resistivity data:

1. Data review. The IP data was reviewed and edited prior to preparing pseudosections and preparing the data sets for inversion. Duplicate readings were averaged and duplicates removed from the data base to leave only a single reading at each station and separation. Readings with large errors which did not repeat within 10% were deleted from the data base.

2. Pseudosection plotting. Pseudosections of the apparent resistivity, chargeability and error in chargeability were prepared from the final edited data. The chargeability, error in chargeability and resistivity sections were scaled to the range on each line. The apparent resistivity in the pseudosections has been corrected for the proximal infinite electrode location.

3. Data formatting. The apparent chargeability, resistivity (in normalized V/I) and topographic data were formatted for entry into the UBC inversion program.

4. Resistivity modelling. For each line, errors in the apparent resistance (V/I) were assigned to the data. There is no means of directly quantifying these errors because neither the transmitter nor receiver record the apparent error in the current or voltage. Errors were assumed to be 0.0005 + 5% ohms. Following error assignment, the data was inverted using these error values. The default mesh is quite adequate for the data set because of the low relief along the survey lines. The default initial and reference models are based on an average of the apparent resistivity. After the default run, the data was inverted a second time using initial and reference models which were 10,000 ohm-m (a much higher value than the average 200-500 ohm-m in the survey area). The purpose of this second run was to generate a model with a background resistivity which was greatly different than the average values used in the default run. After the second run, the two models were compared and regions which showed more than 20% discrepancy were blanked out in the final models. In these blanked out regions, the final models are not sensitive to the field data and no reliable subsurface information is likely contained in these portions of the models.

5. Chargeability modelling. For each line, the observed standard deviation in the chargeability was used as a measure of error in the observed apparent chargeability. The IP data was first inverted using default values. The same mesh used in the resistivity modelling and the final DC resistivity model was used in the IP inversion together with default initial and reference chargeability models. After the first run, the data was inverted a second time using initial and

reference models which incorporated background chargeabilities of 100 mV/V (a much higher value than the average 0-10 mV/V in the survey area). The two models were then compared and regions which showed more than 20% discrepancy were blanked out in the final models. In these blanked out regions, the final models are not sensitive to the field data and no reliable subsurface information is likely contained in these portions of the models.

6. Image extraction. After the modelling was complete, data ranges were compiled and overall data scales were assigned for both the resistivity and chargeability models. A resistivity scale covering the range from 30 to 5000 ohm-m was used as a standard scale for all resistivity models. A consistent scale of 0 to 80 mV/V was used in the chargeability model sections. Several lines contain small regions with modelled chargeability in excess of the maximum value. Final images were generated with the inversion software and converted to JPEGs without further editing. These images are appended to this report in both Appendix E and on CD-ROM.

8. Digital archive. The final IP data and digital copies of the pseudosections and inversions were written to CD-ROM.

Final digital data is appended to this report in Excel spread sheet format. Readings with unacceptable errors and which did not repeat have been deleted from this final data set. Also included is a data base with the line locations. All station locations are shown in UTM coordinates, NAD 1983 datum, Zone 7N projection.

15.0 IP INTERPRETATION METHOD

The data was interpreted using the DCIP2D package developed by the University of British Columbia Geophysical Inversion Facility. The inversion algorithm is described in detail by Oldenburg and Li (1994). A brief description of key features of the algorithm follows.

Siegel (1959) described the IP effect in macroscopic terms. If a time domain signal is put into the ground, as soon as the current is turned on, the voltage immediately rises to a level (ϕ_σ) and thereafter continues to rise to a higher level (ϕ_η). At current shutoff, the voltage immediately falls to a level (ϕ_s) and then slowly decays to zero along a curve similar to that between ϕ_σ and ϕ_η . Apparent chargeability is defined as the "extra" voltage observed:

$$\eta_a = \frac{\phi_\eta - \phi_\sigma}{\phi_\eta} = \frac{\phi_s}{\phi_\eta}$$

The observed DC potentials ϕ_σ are defined by the vector form of Ohms Law:

$$\nabla \cdot (\sigma \nabla \phi_s) = -I\delta(r - r_s)$$

where **r-r$_s$** is the vector to the measurement point, **I** is the current and σ is the conductivity structure of the earth - the unknown quantity in the geophysical problem. The chargeability can be modeled by replacing the conductivity by an equivalent apparent conductivity controlled by the chargeability:

$$\sigma_\eta = \sigma(1 - \eta)$$

Modeling the IP effect then involves running two conductivity models - one with σ and one with σ_η .

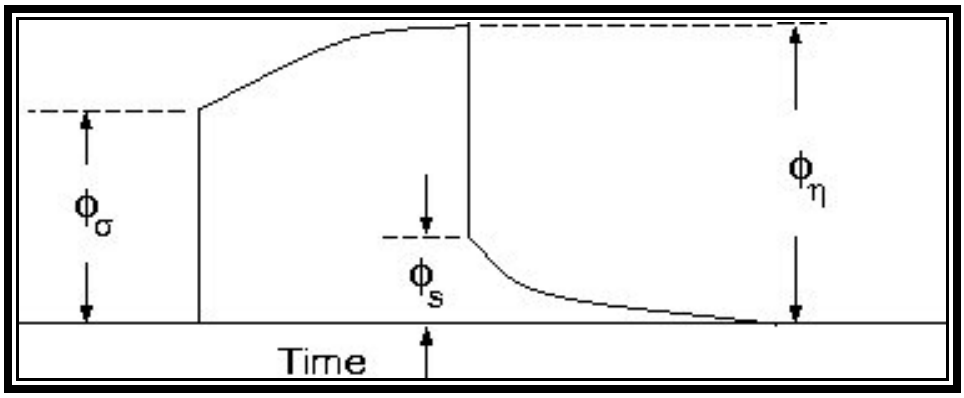

IP response curve (UBC DCIP2D documentation, 1998)

The unknown quantity is the distribution of conductivities in the earth. The software models the earth conductivity structure as a series of rectangular cells of varying size and aspect ratio. The grid is finest (most detailed) near the measurement points and much coarser at locations beside or at depth beneath the measurement points. These cells are necessary to avoid having edge effects appear in the model. The size and dimensions of the models in no way compensates for the basic limitations on depth penetration and resolution inherent in the IP/resistivity survey. Thus the effective depth of penetration (0.5 to 1.0 times the maximum dipole separation) is the limit to which the models should be relied upon to accurately reflect true earth conductivities and chargeabilities.

The program calculates the potential across the finite element network using a starting model. Appropriate boundary conditions are applied when calculating the potentials across the network. These include the condition that all current flow is normal to the cell boundaries and voltages are continuous across the boundaries. The sensitivity of the

model to changing the parameters in any cell is calculated as is the misfit between the model results and the actual observed potentials / chargeabilities. The model is then adjusted using the calculated sensitivities of the response to changes in the conductivity of individual cells.

There is no unique solution or model which fits any set of IP / resistivity data. A best-fit model is one which (1) minimizes misfit and (2) invokes the minimum required degree of complexity to fit the data. The minimization of misfit requires that the sum of the least squares differences between the field data and the data predicted by the model is minimized. For a set of **N** measurements, a global misfit can be defined as:

$$\Psi_d = \sum_{i=1}^{N} \left(W_i(r_i - r_i^{obs})\right)^2$$

where W_i is the weighting factor for the i^{th} measurement (r^{obs}) and r_i is the model response for this measurement. The weighting factor is usually in the order of the inverse of the expected error so that a measurement with high error has a low weighting and vice versa. In a system with no noise and perfectly determined errors, the global error would be **N** because the weighting would compensate for large spreads between model and observed results at points with large errors. The program minimizes Ψ_d by repeatedly adjusting the conductivities to improve the fit.

The second requirement of a successful solution is that the complexity of the final model be minimized. IP measurements are inherent averages, deriving resistivity and chargeabilities from large volumes of the subsurface. It is possible to over model data, deriving solutions which minimize misfit but which invoke models with detail beyond the resolving power of the measuring arrays. Models which incorporate complex detail are inherently ambiguous in that they any number of such models, each with minor variations, may also minimize global misfit. The fine structures in models with extreme complexity exert little or no control on the overall model response. If both a simple and complex solution can adequately replicate the field data within the bounds of measurement error, the simple solution is to be preferred.

Starting with a reference model m_0 and weighting functions for x and z (w_x, w_z), define the complexity of the model as Ψ_m where:

$$\psi_m(m, m_0) = \alpha_s \int\int w_s(x,z)(m-m_0)^2\,dx\,dz + \int\int \left\{ \alpha_x w_x(x,z)\left(\frac{\partial(m-m_0)}{\partial x}\right)^2 + \alpha_z w_z(x,z)\left(\frac{\partial(m-m_0)}{\partial z}\right)^2 \right\} dx\,dz$$

where α_x , α_z and α_s define the relative weight of the model in x, z and fineness.

Increasing any of these values beyond their normal values of 1.0, 1.0 and 0.001, increases the importance of that dimension in the final solution. For example, to weight the final solutions towards vertical structures, α_z would be weighted several times more than α_x. To force the model to generate fewer small scale structures, α_s is increased.

The final criteria for a successful solution can then be expressed as:

1. Minimize Ψ_m

2. Subject to the constraint that Ψ_d = N (or very close to it).

Consequently, the inversion process seeks to minimize two loosely related functions. To evaluate a solution, the reader should examine not only the final values but the path the program followed to reach these values. An example of typical convergence curves is shown below. The black line traces the value of Ψ_d with each iteration and in a good inversion, this will converge to the target misfit (N). The orange curve traces the convergence behavior of Ψ_m . This curve normally starts at a very small value because the reference model is usually set to the initial model and the initial and reference models are very simple. As the inversion proceeds, the solution model becomes increasingly complex as it is adjusted to meet the target misfit. After reaching target misfit, minor adjustments are made to reduce the complexity of the model and the Ψ_m curve stabilizes at some high value.

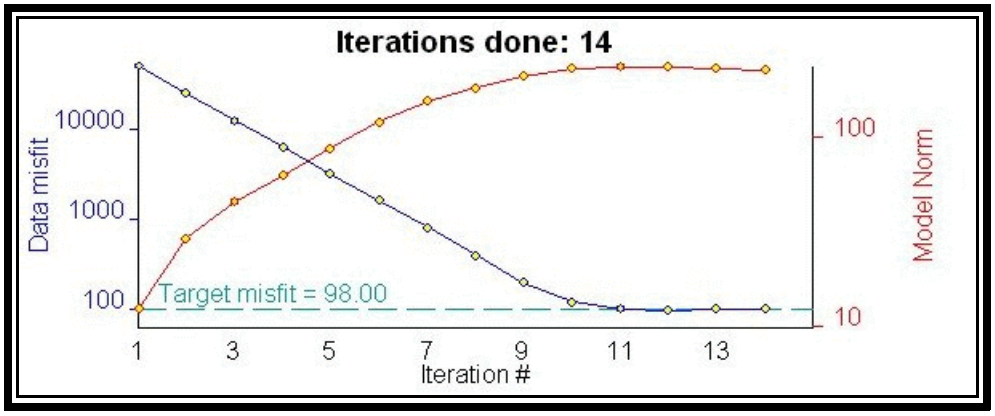

Typical convergence curves - DC inversion

The field observations often have significant poorly quantified errors and the complexity of the background conductivity response may be such that it is impossible to reduce Ψ_d to N. Instead, Ψ_d can be scaled proportionately by a "chi-factor" ranging up or down from 1.0 (no scaling). Setting a large chi-factor loosens the control that goodness-of-fit exerts on the solution and generally directs the program to use very simple models which tend to smooth out the conductivities and fails to accurately model the fine details in resistivity or chargeability known to exist in the ground. Setting a chi-factor which is too low may prevent convergence to an acceptable solution. Generally, chi is left at 1.0.

A final feature of note in the inversion is the use of initial and reference conductivity and chargeability models in the inversion process. As noted above, the relation for Ψ_m requires a reference model (m_0) against which solutions are compared. This can be an actual 2D model constructed from known geology or a estimate of half space conductivity or chargeability. In addition, the modeling process will start from an initial model which has the same general form. In general, an average half space conductivity and chargeability based on the field values is the best model to start from and this is the default model for both inversions if none other is specified. This will ensure that Ψ_m converges to a value which is not too large. The initial and reference models can be used to estimate the depth of investigation. If two inversions are performed with very different reference models, there will be regions in the final models which will be the same in both inversion and peripheral regions where the final models will resemble the reference models. An example is shown below:

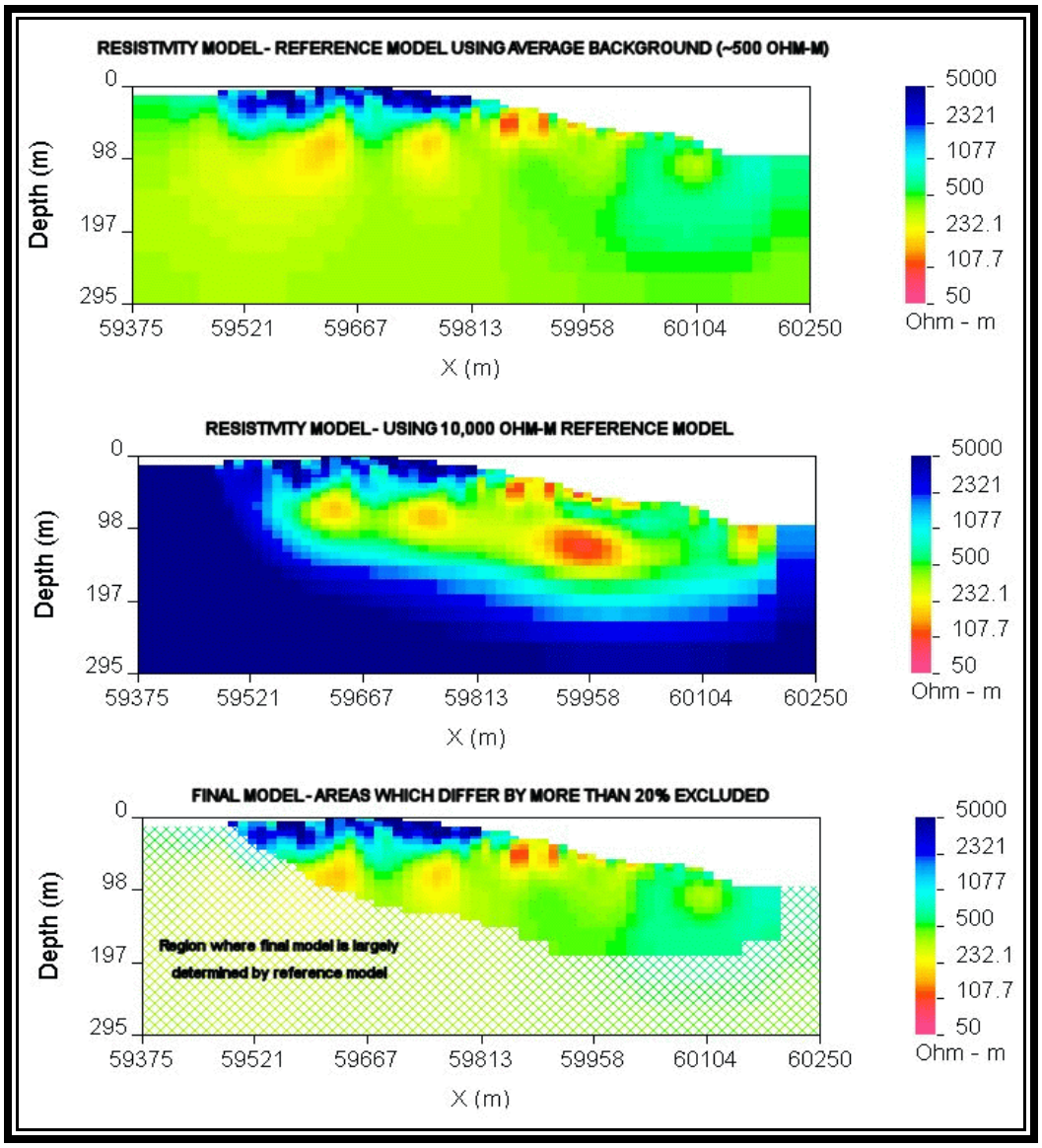

Depth of investigation determined from inversion results using different initial and reference models.

15.0 RESULTS

The results of the geophysical survey program are discussed by method.

Gravity

A summary of the gravity data and reductions is contained in Appendix D. Figures 5 and 6 (Back pocket) are Bouguer Anomaly maps showing the colour contoured reduced gravity data (Figure 5) and the Bouguer Anomaly together with topography (Figure 6). A digital archive is appended to this report as a CD-ROM and contains the gravity data in Excel and Geosoft data base format. The archive also contains all raw GPS and gravity data , near station terrain measurements, the digital model used in the corrections and a digital copy of the report and Bouguer Anomaly map.

The central gravity feature on the property is a large Bouguer high running NNW-SSE and centred largely in low ground NE of the ridge on which the mineralization is found. This anomaly, approximately 3 to 4 mGal in amplitude terminates immediately west of Shell Creek. The anomaly is a long wavelength feature with a half-width of approximately 6 km.

The Bouguer Anomaly data collected during this survey were inverted to investigate the density, depth and shape of the source body or bodies creating the observed field. The gravity modelling was confined to the area bounded by 517000E 7154000N to 537500E 7174000N. The regional field was removed by subtracting 5336.894 mGal from the data set to yield a data set with a base level of 0.0 mGal in the valley of the Yukon River (the lowest gravity readings in the survey area). Topography was gridded using 100 m cells in the same area and used to truncate the mesh, thereby incorporating surface topography into the final model. Modelling was conducted to fit the 46 points within the model area rather than attempting to fit a grid derived from this data. The model employed grid cells 200 m x 200 m in plan and 100 m thick near surface. The inversion was conducted with default (1.0) chi-factors, default α's and with default z_0 and β coefficients to counteract depth insensitivity. Reference and initial models consisted of cells with a zero density contrast.

The inversion fitted the data within 0.5 mGal throughout most of the survey area. Figure 7 illustrates the observed gravity data (a), the gravity data predicted by the best-fit model (b) and the difference between the observed and predicted gravity (c). The inversion failed to accommodate the high gravity observed at stations near the north edge of the model - a result which is to be expected in this instance as the anomaly trends out of the area containing the model and it would be difficult to accommodate this gradient without excess mass well beyond the modelling limits.

Figure 8 illustrates the final model. The solid shown encloses all material with density

greater than 0.2 g/cm^3 above background (ie. greater than 2.87 g/cm^3 relative to average crustal density of 2.67 g/cm^3). The large scale high is likely generated by a deep-seated crustal feature which does not sub-crop. There are several small, isolated density highs near surface following the axis of the ridge upon which the mineralization is found. Any single cell feature is suspect and may be an artifact of the inversion. The relationship between some of the larger features and the mineralization on the property should be examined to determine their significance. The centre and dimensions of the shallow anomalous regions are summarized in the table below:

Source number	Location (UTM NAD83)	Dimensions (m)
1	527180E 7162500N	800 (EW) x 500 (NS)
2	530970E 7160760N	400 (EW) x 300 (NS)

Anomalous source mass #1 is located on the IP survey grid and its location is shown in Figure 4.

IP / Resistivity surveys

IP pseudosections are included with this report in back pockets. Inversion models are compiled in Appendix E. Digital data and JPEGs of all pseudosections and inversion models are on the CD-ROM. In general, the survey detected very low chargeability and high resistivity throughout the survey area. Line 3200N was surveyed with 50 m dipoles and the resistivity results indicate the presence of numerous thin steeply-dipping low resistivity zones with no associated chargeability response. These features may be present on lines 2000N and 2900N as well but they are not well imaged by the wider dipole spacing.

The most promising anomalies detected are a pair of chargeability highs on Line 2000N. A coincident chargeability high and resistivity low near10600W occurs in a small draw. The source appears to subcrop and is likely steeply dipping although the geometry is not well imaged in the inversion. A deeper chargeability high centred at about 9500W is marginal to a resistivity low immediately to the east. The source body appears to be at least 100 m below surface.

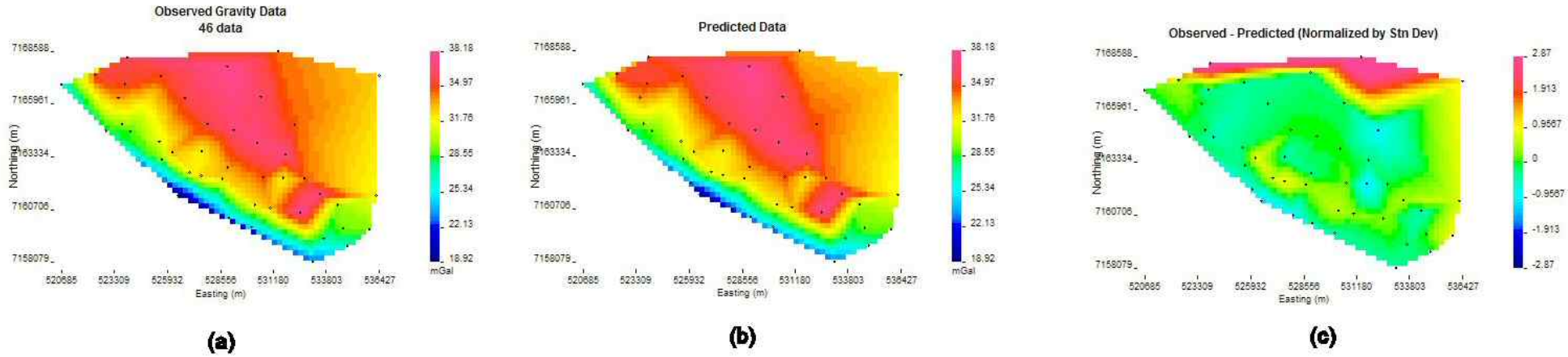

Figure 7. Gravity modeling results. (a) Observed Bouguer anomaly in model area. (b) Bouguer anomaly predicted by the final best-fit model (c) difference between the observed and model gravity in mGal

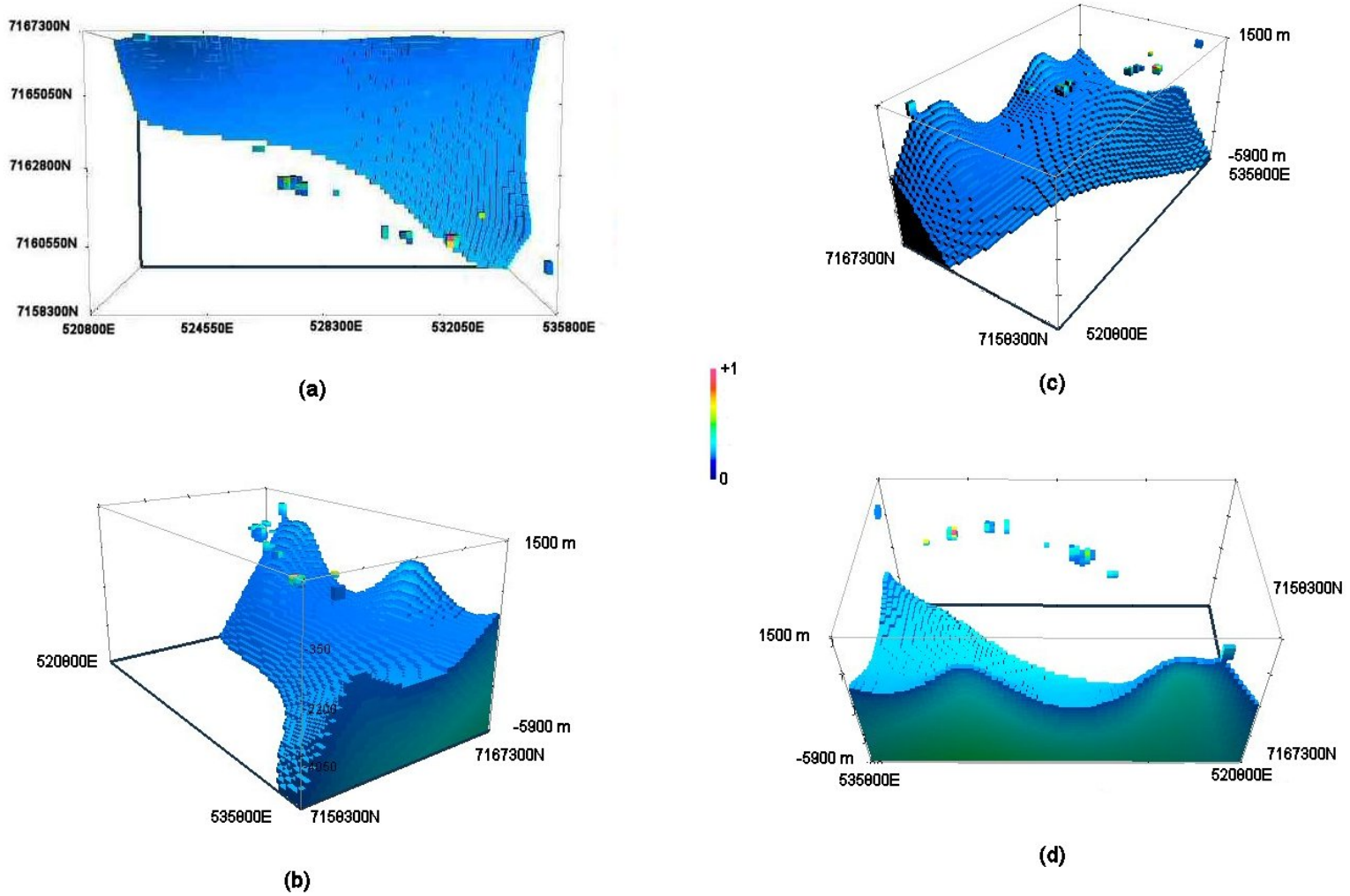

Figure 8. Gravity model. Perspective views of the best-fit gravity model. Surface shown encloses all material with density greater than 2.87 g/cm3. Density values of each exposed node are color coded according to the color scale bar, ranging from 2.67 to 3.67 g/cm3 (0 to +1.00 g/cm3 above average crustal density). Horizontal axes in each view are labelled in UTM NAD83 (Zone 7N) coordinates and the elevations shown are metres relative to mean sea level. (a) Top view. (b) View from southeast. (c) View from southwest (d) View from north.

16.0 CONCLUSIONS

The results of the geophysical surveys support the following conclusions:

a. A prominent, NW-SE trending, regional scale, 3 to 4 mGal gravity high occurs in the northern portion of the property. The axis of the high is north of the ridge upon which known copper-gold mineralization is found.

b. The large gravity high appears to be caused by a deep seated density high with a density contrast in the order of 0.2 to 0.5 g/cm^2.

c. Smaller shallow density highs are located in the area of where the copper gold mineralization is found. Neither is associated with anomalous IP or resistivity response.

d. The IP survey detected low chargeabilities across the survey grid with the exception of two anomalies on the west end of L2000N. A shallow coincident resistivity low and chargeability high is centred near 10600W. The anomaly occurs in a small draw or re-entrant.

17.0 RECOMMENDATIONS

The conclusions support the following recommendations:

a. The chargeability anomaly on L2000N at 10600W should be investigated by surface prospecting and trenching.

b. High frequency HLEM surveys should be tried along the IP lines to attempt to locate mineralized structures. The presence of thin resistivity lows with no coincident chargeability anomalies in the short-dipole data from L3200N suggests that this approach may be more useful than IP in this setting.

Respectfully submitted,
AURORA GEOSCIENCES LTD.

Mike Power M.Sc. P.Geoph.
Geophysicist

REFERENCES CITED

Ash, C (2005). Shell Creek property geology. www.loganresources.com

Coggon, J.H. (1973). A comparison of IP electrode arrays. Geophysics Vol. 38, No 4. pp 737-761.

Gordey, S.P. and A.J. Makepeace (1999) Yukon Digital Geology, Open File D3826. Geological Survey of Canada: CD-ROM.

Hanneson, J.E. (1990) A model for interpreting IP/resistivity data from areas of steep dip and thin overburden. in: Fink, J.B. *et. al.* (ed.) Induced polarization: applications and case histories. Tulsa: Society of Exploration Geophysicists.

Hohmann, G.W. (1990) Three-dimensional IP models. in: Fink, J.B. *et. al.* (ed.) Induced polarization: applications and case histories. Tulsa: Society of Exploration Geophysicists.

Johnson, I.M. (1990) Spectral IP parameters derived from time domain measurements. in: Fink, J.B. *et. al.* (ed.) Induced polarization: applications and case histories. Tulsa: Society of Exploration Geophysicists.

LaFehr, T.R. (1991a) Standardization in gravity reduction. Geophysics Vol. 56, No. 8. pp 1170-1178.

LaFehr, T.R. (1991b) An exact solution for the gravity curvature (Bullard B) correction. Geophysics Vol. 56, No. 8. pp 1179-1184.

Longman, I.M. (1959) Formulas for computer the tidal accelerations due to the moon and the sun. Journal of Geophysical Research Vol. 64 No. 12.

Oldenburg, D.W. and Y. Li (1994) Inversion of induced polarization data. Geophysics Vol. 59. No. 9. pp. 1327-1341.

Sumner, J.S. (1976) Principles of Induced Polarization for Geophysical Exploration. New York: Elsevier.

Telford, W.M., L.P. Geldart and R.E. Sheriff (1990) Applied Geophysics (2nd Edition) New York: Cambridge University Press.

Whitman, W.W. (1991) A microgal approximation for the Bullard B - earth's curvature - gravity correction. Geophysics Vol.56 No. 12 pp 1980-1985.

APPENDIX A. CERTIFICATE

I, Michael Allan Power, M.Sc. P.Geo., P.Geoph., with business and residence addresses in Whitehorse, Yukon Territory do hereby certify that:

1. I am a member of the Association of Professional Engineers and Geoscientists of British Columbia (registration number 21131) and a professional geophysicist registered by the Northwest Territories Association of Professional Engineers, Geologists and Geophysicists (licensee L942).

2. I am a graduate of the University of Alberta with a B.Sc. (Honours) degree in Geology obtained in 1986 and a M.Sc. in Geophysics obtained in 1988.

3. I have been actively involved in mineral exploration in Northern Canada and Alaska since 1988.

4. I have no interest, direct or indirect, nor do I hope to receive any interest, direct or indirect, in Logan Resources Ltd. or any of its properties.

Dated this 12th day of November, 2005 in Whitehorse, Yukon.

Respectfully Submitted,

Michael A. Power M.Sc. P. Geoph.

APPENDIX B. SURVEY LOG

AURORA GEOSCIENCES LTD.

SHELL CREEK GRAVITY
JOB LGR-05-01-YT
LOGAN RESOURCES LTD.

Period: June 8th - June 13th , 2005

Personnel:
Mike Power (MP) - Geophysicist / crew chief
Carla Kennedy (CK) - Geophysicist / tech

Wed 8 June 05 Mobe
Packed gear, completed DTM, left Whitehorse at 1300 hrs. Arrived Dawson around 1900 hrs. Checked in to Bonanza Gold Hotel.
Wx: sunny & warm.

Thu 9 June 05 Survey
Met at TNTA at 0740. Initial gravimeter check-in (local station at hangar) and safety briefing followed. Left for property at 0815 hrs. Set up base station GPS at a geodetic marker and established a survey gravity base station nearby. Surveyed a couple of stations on foot while the IP crew was mobilized to the property. Thereafter, began helicopter surveying. Demobe of linecutters, IP crew and gravity crew began at 1700 hrs. Crew back in Dawson at 1930 hrs.
Wx: sunny & warm

Production: 23 stations

Fri 10 June 05 Survey
Met at TNTA at 0730 hrs, arrived on site around 0830 hrs. Line cutters were late in arriving and arrived in two groups; consequently only 2 on-foot points covered before the helicopter was released for gravity work at 1130 hrs. Demobe of line cutters, IP crew and gravity crew began at 1700 hrs; arrived back in Dawson around 1900 hrs.
Wx: sunny with afternoon buildup and thundershowers; warm.

Production: 18 stations

Sat 11 June 05 Survey
Met at TNTA at 0730 hrs and departed with Mark Terry and Chris Ash (geologists). Helicopter freed for work around 1100 hrs after moving in the line cutters. Completed survey, tore down gear and took everything back to Dawson. Wx: sunny in AM, afternoon buildup, thundershowers with hail, rain and lightning.

Production: 19 stations

Sun 12 June 05 Data processing
Stayed in Dawson, processed data and generated interim map. Wx: heavy afternoon thundershowrs.

Mon 20 June 05 Demobe
Left Dawson at 1300 hrs, arriving Whitehorse at 1900 hrs.
Wx: sunny & warm

Total Production: 60 stations
Survey: 3 days

AURORA GEOSCIENCES LTD.

SHELL CREEK IP
JOB LGR-05-02-YT

Period: June 3rd - June 16th, 2004

Personnel:

Dave Hildes (DH)	Crew Chief
Casey Adshead (CA)	Technician
Andrea Langerud	Helper
Calvin Delwisch	Helper

Fri June 03 05 Mobe

Meet at 0700, pick up groceries, drive to Dawson and onto camp site. Set up camp at 519373, 71422088 (UTM zone 7, NAD83) next to the 40 mile river.

Sat June 04 05 Survey

Late start as there was a delay in Dawson and waited for the helicopter (1.5 hours late). First flight at 1020 with Tx gear, needed two flights this morning. CD on cables, DH on Current, AL on Tx, CA on Rx. Some holes in data because of deep snow pockets. Data generally of good quality, with low chargeabilities. Back in camp at 1800 in one flight.
Wx: Sunny, cool (15 deg C), windy (up to 40-50 km/h).

Production: 1075 m

Sun June 05 05 Survey

Late start again as we had to wait for helicopter until 1000 for pickup. CA on cables, DH on current, CD on Tx and AL on Rx. Bad weather starts to move in and have to fly out early. Back in camp at 1520.
Wx: Overcast, cool, fog.

Production: 900 m

Mon June 06 05 Survey

Fog in Dawson, helicopter delayed until 1020. AL on cables, DH on current, CD on Tx and CA on Rx. Requires a Tx move halfway through the day to maintain radio communications. No problems, but survey a little slow because of steep topography. Back in camp at 1845.

Wx: Morning fog, scattered showers, cool (10-15 deg C).

Production: 1375 m

Tue June 07 05 Weather Day
By noon, the fog had cleared at camp elevation, but the property remained in cloud. Pilot cancelled all flights for the day. Client requested 100 m cables, drive to Brewery Creek (5 hours return) to collect 100 m cables in the afternoon.
DayWx: Low morning fog, both at camp and in Dawson.

Production: 0 m

Wed June 08 05 Survey
Again wait until 1015 for helicopter. At the request of client, try 50 m dipoles for the rest of the line. CD on cables, DH on current, AL on Rx and CA on Tx. Complete L3200N and begin to clean some current wire from line. Back in camp at 1815.
Wx: Clear, hot (25 deg C), some wind.

Production: 2050 m

Thu June 09 05 Survey
Continue 50 m dipoles on L3200 N, reading west from 3200 to go over known mineralized zone. DH on cables, AL on current, CA on Rx and CD on Tx. Lose radio contact with Tx at 4700, and then clean the line. Back in camp at 1825.
Wx: Clear, hot (27 deg C), windy. Pick up at 0900.

Production: 1700 m

Fri June 10 05 Survey
Pick up at 0900. Transfer all gear to L2000 and put Tx on the east side of line and set up with 100 m cables. CA on cables, CD on current, DH on Tx and AL on Rx. Survey proceeds well but line cutters were not as far ahead as they had expected so the afternoon became very slow as we had to wait for line to cut ahead of us. Very hot, some problems with minor heat stroke. Thunderheads develop in afternoon, helicopter has a hard time. Back in camp at 1700.
Wx: Clear, hot, thunderstorms in afternoon.

Production: 1600 m

Sat June 11 05 Survey
Move Tx to L2900, survey with 100 m dipoles. DH on cables, CD on current, CA on Tx, AL on Rx. Survey proceeds well, but the line was not cut beyond 4500. Surveyed until station 4700 then bush became too thick and the line was abandoned Clean line and wait for helicopter to be available for pick-up. Back at camp at 1800.
Wx: Clear, hot, thunderstorms in afternoon. Pick up at 0845.

Production: 2300 m

Sun June 12 05 Survey Day
Last crew out today, late start: pick up at 1015. Move Tx to L2000, at a different location than June 11. Set up is slow because Tx location is not ideal. DH on cables, CD on current, AL on Tx and CA on Rx. Hard time getting good current into the ground, very noisy data. Strong winds develop late in afternoon, pilot begins to pull the crews out at 1700. Everybody back at camp 1830.
Wx: Clear, hot, thunderstorms in afternoon.

Production: 1000 m

Mon June 13 05 Survey
Helicopter late because of fog in Dawson, out at 1015. DH and CD pick up some wire at the start of the line while CA and AL lay out cables. Begin survey with CD on cables, CA on current, DH on Tx and AL on Rx. Needed to move the Tx to maintain radio contact halfway through the day. Move into ground better for currents, improving the signal to noise. Back at camp at 1910.
Wx: Clear, hot, storms in the late afternoon.

Production: 2000 m

Tue June 14 05 Survey
Pick up at 0815, continue work on L2000N. AL on cables, DH on current, CD on Tx and CA on Rx. Complete and clean L2000N. Many pickets are mislabelled, ignore them by end of day. Back in camp at 1830.
Wx: Clear, hot.

Production: 1700 m

Wed June 15 Survey
Work on L2900N, the line was fixed yesterday. DH on cables, CD on current, AL on Tx and CA on Rx. Complete and clean L2900. Move all gear back to camp in 2 loads, back at 1900. Pick up at 0815.
Wx: Clear, warm, windy.

Production: 2700 m

Thu 16 June Demobe
Drive back to Whitehorse.

Sun Sept 11, 05 Survey.
Late start due to fog in Dawson. Conditions of IP line are steep terrain with some thick bush, line should be cut for job to be done properly. Continued without linecutting but job will take two days rather than the anticipated one. PJ & WK

fly out with one internal load. CA & TS drive to 40 mile and mobe in rest of gear with one more internal load. ~2 ½ to 3 hrs to establish line. Production: 700m IP survey. Plan to leave truck at 40 mile and finish job tomorrow. Emergency landing in heli on flight home, luckily it occurred right near 40 mile and pilot able to put down on road. Main rotor blades damaged as trees were struck on landing. Crew drives back to town, in by 10 pm everyone ok. Plan to continue shell job with replacement jet ranger from Mayo.

Mon Sept 12, 05 Survey

Replacement jet ranger in by 10:30 am. PJ & TS out to site by 11:30. WK & CA drive truck back out to 40 mile, mobe in from there. IP line completed. All crew mobe out through truck at 40 mile. One sling load and one ferry flight required to 40 mile. Crew in town by 7:15 pm. Weather clear. Long Ranger still down at 40 mile.

Total Production: 19.8 line-km

Survey Days: 13.0 days
Standby Days: 1.0 days
Mobe/Demobe: 2.0 days

APPENDIX C. INSTRUMENT SPECIFICATIONS

APPENDIX D. GRAVITY MEASUREMENTS & REDUCTIONS

APPENDIX E. IP / RESISTIVITY INVERSION RESULTS

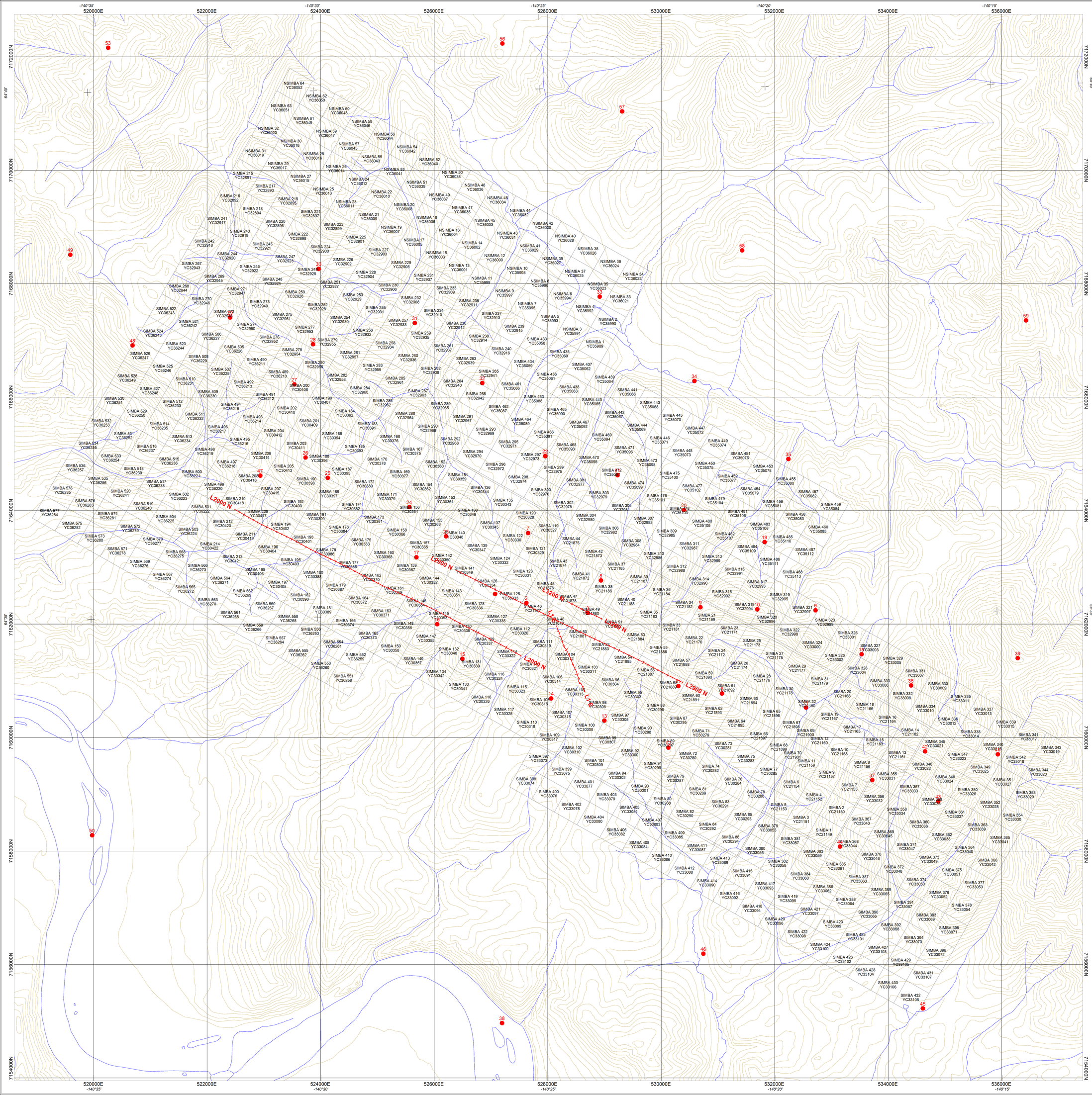

LOGAN RESOURCES LTD.

SHELL CREEK
2005 GEOPHYSICAL SURVEY
FIGURE 2. CLAIMS AND SURVEY LOCATION MAP

NTS: 116C09/10
Datum: NAD83
Date: November 8 2005

MINING DISTRICT: DAWSON
Projection: Zone 7N
Job: LGR-05-01-YT /LGR-05-02-YT

AURORA GEOSCIENCES LTD.

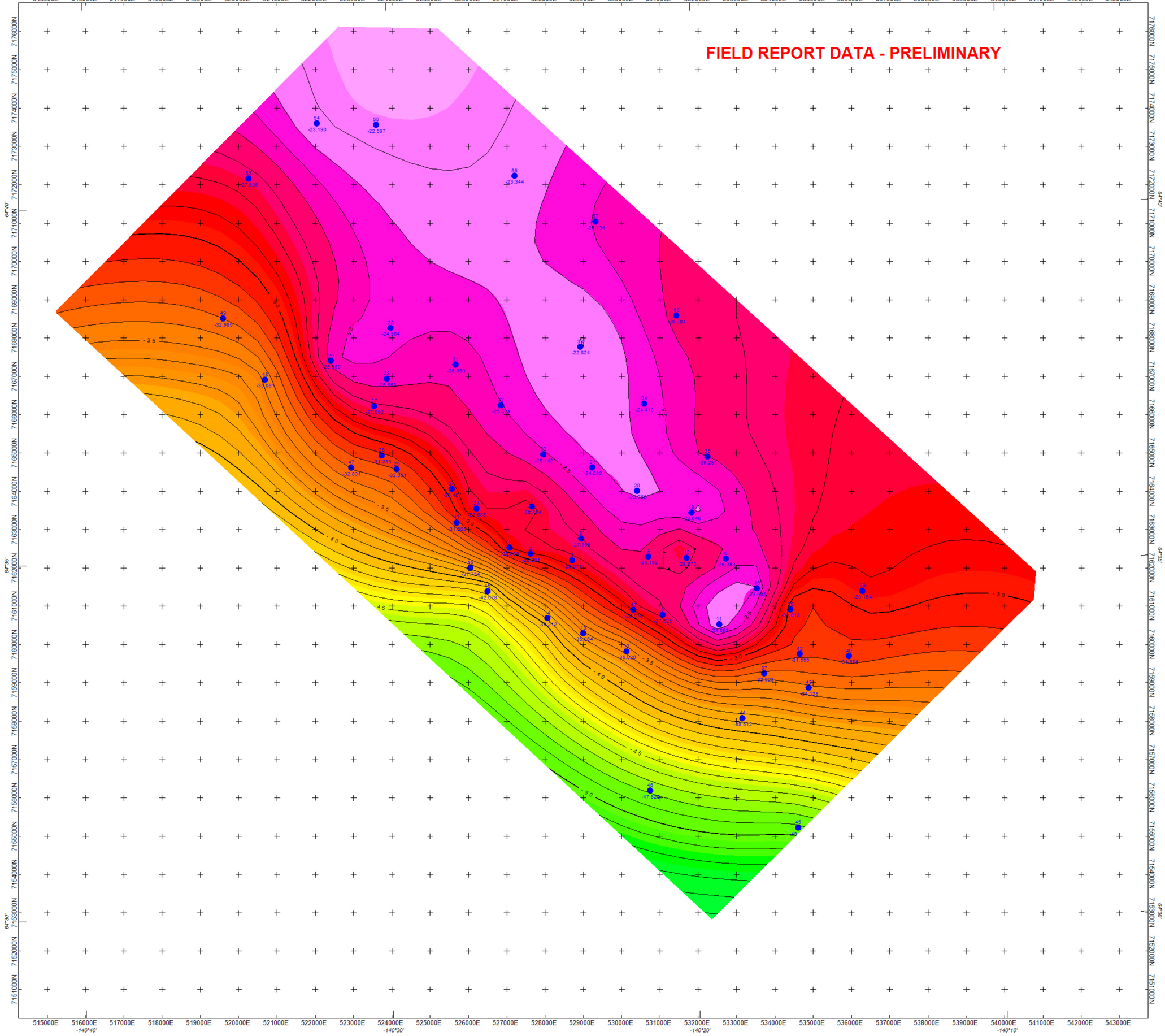

-22.500
-24.000
-25.000
-26.000
-27.500
-28.500
-29.500
-31.000
-32.000
-33.000
-34.000
-35.500
-36.500
-37.500
-39.000
-40.000
-41.000
-42.500
-43.500
-44.500
-45.500
-47.000
-48.000
-49.000
-50.500
-51.500
-52.500
-54.000
-55.000
-56.000
-57.000
-58.500
-59.500
-60.500
-62.000
-63.000
-64.000
-65.000

Bouguer Anomaly (GSC Levelled)
(mGal)

LEGEND

BOUGUER GRAVITY

CONTOUR INTERVALS (mGal)

1.0
5.0
10.0

DATUM : GSC
INSTRUMENT : Scintrex CG-5
GRIDDING ALGORITHM : MINIMUM CURVATURE
GRID CELL SIZE : 500 m
FILTER : nil
FILTER SPECS : nil
DATA FILE : Shell Creek - Final gravity.gdb
STATION SEPARATION : Average 1000 m
POINTS SURVEYED THIS SHEET : 60

GRAVITY DATA REDUCTIONS

1. DRIFT CORRECTION: GRAVITY BASE STATION AT UTM (ZONE 7N) 526415.7E 7162784.9N; NOMINAL DATUM 5345.666 MGAL.
2. GPS BASE STATION AT GEODETIC SURVEY OF CANADA MONUMENT # 65A44 USING POSTED ELEVATION ABOVE MEAN SEA LEVEL 1378.9 M.
3. LATITUDE CORRECTION: GRID CENTRE AT 528000E 7172000N, LATITUDE AT GRID CENTRE 64.582N; UTM DECLINATION 0.62 E.
4. ELEVATION CORRECTIONS: FREE AIR, BOUGUER SLAB, BULLARD-B USING MEAN SEA LEVEL AS DATUM AND A CORRECTION DENSITY OF 2.67 G/CM**3.
5. TERRAIN CORRECTIONS PERFORMED SOLELY WITH A 25 M DTM EXTRACTED FROM LOCAL TOPOGRAPHY AND' INCORPORATING MEASURED STATION ELEVATIONS.
6. FINAL DATA LEVELLED TO GSC GRAVITY DATUM BY SUBTRACTING 5397.000 MGAL FROM FINAL CORRECTED GRAVITY.

Scale 1:50000

1000 0 1000 2000 3000
metres
NAD83 / UTM zone 7N

LOGAN RESOURCES LTD.

SHELL CREEK PROJECT
Gravity Survey
Bouguer Anomaly Map

NTS: 116 C 9/10
Datum: NAD83 (Canada Mean)
Job: LGR-05-01-YT

Mining District: Dawson
Projection: UTM Zone 7
Date: 16 June 2005

AURORA GEOSCIENCES LTD.

FIELD REPORT DATA - PRELIMINARY

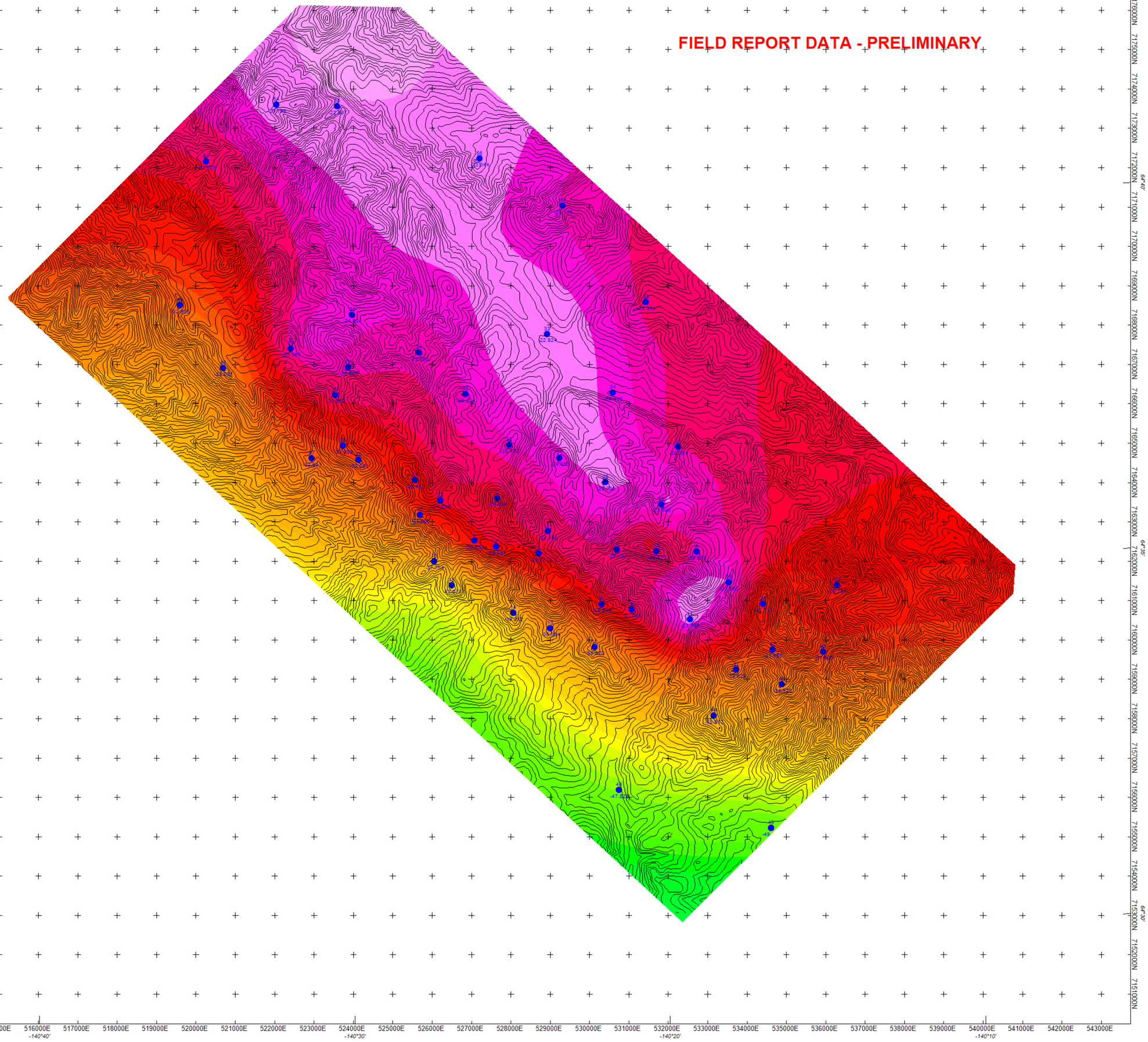

-22.500
-24.000
-25.000
-26.000
-27.500
-28.500
-29.500
-31.000
-32.000
-33.000
-34.000
-35.500
-36.500
-37.500
-39.000
-40.000
-41.000
-42.500
-43.500
-44.500
-45.500
-47.000
-48.000
-49.000
-50.500
-51.500
-52.500
-54.000
-55.000
-56.000
-57.000
-58.500
-59.500
-60.500
-62.000
-63.000
-64.000
-65.000

Bouguer Anomaly (GSC Levelled)
(mGal)

Scale 1:50000

1000 0 1000 2000 3000
metres
NAD83 / UTM zone 7N

GRAVITY DATA REDUCTIONS

1. DRIFT CORRECTION: GRAVITY BASE STATION AT UTM (ZONE 7N) 526415.7E 7162784.9N; NOMINAL DATUM 5345.666 MGAL.
2. GPS BASE STATION AT GEODETIC SURVEY OF CANADA MONUMENT # 65A44 USING POSTED ELEVATION ABOVE MEAN SEA LEVEL 1378.9 M.
3. LATITUDE CORRECTION: GRID CENTRE AT 528000E 7172000N, LATITUDE AT GRID CENTRE 64.582N, UTM DECLINATION 0.62 E.
4. ELEVATION CORRECTIONS: FREE AIR, BOUGUER SLAB, BULLARD-B USING MEAN SEA LEVEL AS DATUM AND A CORRECTION DENSITY OF 2.67 G/CM**3.
5. TERRAIN CORRECTIONS PERFORMED SOLELY WITH A 25 M DTM EXTRACTED FROM LOCAL TOPOGRAPHY AND' INCORPORATING MEASURED STATION ELEVATIONS.
6. FINAL DATA LEVELLED TO GSC GRAVITY DATUM BY SUBTRACTING 5397.000 MGAL FROM FINAL CORRECTED GRAVITY.

LOGAN RESOURCES LTD.

SHELL CREEK PROJECT
Gravity Survey
Bouguer Anomaly Map (GSC levelled) with topography

NTS: 116 C 9/10
Datum: NAD83 (Canada Mean)
Job: LGR-05-01-YT

Mining District: Dawson
Projection: UTM Zone 7
Date: 16 June 2005